SCHOOL OF GRADUATE STUDIES

COLLEGE OF TECHNOLOGY AND BUILT ENVIROMENT

CENTER FOR RENEWABLE ENERGY TECHNOLOGY

Thesis on

Design and Manufacturing of Small-Scale Wind Turbine Blade for Rural Electrification using Banana Fiber.

By

Hassan Rashid Issack (GSR/7525/16)

Advisor

Mesfin Belayneh (PhD)

February, 2026

Addis Ababa, Ethiopia

Addis Ababa University

College of Technology and built Environment

Center for Renewable Energy Technology

"Design and Manufacturing of Small-Scale Wind Turbine Blade for Rural Electrification using Banana Fiber".

By

Hassan Rashid Issack

Approved by Bord of Examiners

Mesfin Balaynh (PhD)	[signature]	05/03/26
Advisor	Signature	Date
Solomon T/mariam (PhD)	[signature]	05/03/26
Internal Examiner	Signature	Date
Wondwossen Bogale	[signature]	05/03/26
External Examiner	Signature	Date
Ebrahim T/[illegible] (PhD)	[signature]	06/03/2026
Chairman	Signature	Date
------------------------	------------	----------
Director, Postgraduate program	Signature	Date

Addis Ababa University College of Technology and Built Environment — Vice Executive Dean Office for Academic Affairs

ACKNOWLEDGMENT

I would like to give Glory to Allah; I know any work wouldn’t last without Allah ‘s will. I would like to express my deepest gratitude to my dear instructor and advisor, Dr. Mesfin Belayneh for his professional guidance and support in completing this research.

LIST OF FIGURES

LIST OF TABLES

ACRONYMS

a: Axial induction factor

a’: Angular Induction Factor

A: Cross-sectional Area

A_g: Area of the Air gab

B: Blade Numbers

BEM: Blade Element Momentum

BEMT: Blade element Momentum theory

C: Airfoil Chord length

C_L: Coefficient of lift

$C_{D:}$ Coefficient of Drug

$C_{P:}$ Power coefficient

$C_{T:}$ Thrust coefficient

CFD Computational fluid dynamics

EMF: Electromotive Force

FEA: Finite Element Analysis.

HAWT: Horizontal Axis Wind Turbine

NDT: Non-destructive testing

P: Power output (W),

ρ: Air density (kg/m³),

SSWT: Small scale wind turbine

UN: United Nation

UNDP: United Nations Development Program)

ABSTRACT

This paper presents the design, structural evaluation, and manufacturing of a small-scale wind turbine blade developed for rural electrification using natural banana (Enset) fiber reinforced composite material. The blade geometry was created and optimized using SolidWorks simulation. Numerical analysis showed that the maximum stress occurs at the blade root while the maximum displacement occurs at the blade tip, indicating a safe and acceptable deformation pattern. Strength analysis under different operating conditions demonstrated adequate reliability, including yawing load (3.9 MPa, factor of safety 7), yaw error (0.4 MPa, factor of safety 3.7), maximum rotational speed centrifugal loading (1.99 MPa tensile stress, factor of safety 15), short-at-load connection (2.338 MPa, factor of safety 12), shutdown parking (1.1 MPa, factor of safety 15), and parked wind loading (4.07 MPa, factor of safety 7). The manufacturing procedure followed sequential steps: CAD modeling in SolidWorks, prototype fabrication using a 3D printer, preparation of a master pattern, mold fabrication, production of two mold halves, and composite lay-up. The blade was produced using resin matrix reinforced with Enset fiber, polyvinyl (PV), hardener, and gelcoat. The results confirm that the proposed blade is structurally safe, manufacturable, and suitable as a low-cost sustainable solution for decentralized rural power generation.

Keywords: Banana fiber composite, Enset fiber, small wind turbine blade, rural electrification, structural analysis, composite molding, 3D Machine, renewable energy technology.

Contents

CHAPTER ONE

1. INTRODUCTION

Because of the urgent need for sustainable energy sources and the growing concern over climate change, wind energy has grown in importance in the global renewable energy landscape. According to different wind energy technologies, small-scale wind turbines (SSWTs) have grown in popularity, especially for decentralized energy generation in residential and small commercial applications. Turbines with capacities usually under 100 kW are classified as SSWTs and provide several advantages, including reduced installation costs, minimal land requirements, and the potential for customer energy independence (1,2). This increasing interest reflects a broader trend toward renewable energy as communities search for local methods of energy production that reduce reliance on fossil fuels.

Recent improvements in design and manufacturing techniques have significantly increased the efficiency, dependability, and cost-effectiveness of SSWTs. Aerodynamic, structural, and control system innovations have resulted in improved performance and longer operational lifespans(1,2). For example, innovative blade designs based on computational fluid dynamics (CFD) have improved energy capture while also addressing noise concerns, which are critical in urban environments where these turbines are frequently erected (3). Such enhancements not only make SSWTs more competitive, but also increase their acceptance within areas that may be sensitive to environmental consequences.

Advances in design have been accompanied by an evolution in manufacturing techniques towards the adoption of sustainable practices and materials. Production costs and environmental effects related to the construction of turbines have decreased as a result of the usage of composite materials and additive manufacturing processes(4,5). Increased precision and efficiency are made possible by automated processes, which further streamline production. This change in production is in line with the requirement for energy solutions that leave the least possible environmental impact as well as the increased emphasis on sustainability in engineering methods.

Additionally, the integration of smart technologies and Internet of Things (IoT) capabilities has revolutionized the operational efficiency of SSWTs. Real-time monitoring systems enable predictive maintenance, which minimizes downtime and optimizes performance throughout a turbine's lifespan (8,9). These technological advancements are crucial for maximizing energy generation and ensuring small-scale wind turbines operate effectively in a variety of climatic conditions. The adaptability of these smart devices increases the viability of SSWTs in both urban and rural settings.

The most recent discoveries and developments in the design and manufacturing of small-scale wind turbines are the main topics of this literature study. Through case studies, innovative production processes, performance evaluation techniques, and structural and aerodynamic design considerations, the real-world use of SSWTs will be illustrated. By looking at these areas, this analysis seeks to give a comprehensive picture of the state of small-scale wind turbine technology today and its implications for the development of renewable energy solutions.

Finally, advancements in small-scale wind turbine technology offer a promising option for sustainably tackling energy concerns. As communities and governments encourage renewable energy, SSWTs provide a realistic alternative for local wind energy generation This analysis will help to clarify how small-scale wind turbines can be crucial to the shift to a more sustainable energy future by examining recent advancements in design, manufacture, and operational efficiency.

1.2 Statement of the Problem

Access to reasonably priced and dependable electricity is still a major problem in many Ethiopian rural communities. A sizable section of the rural populace still does not have connection to the national grid, despite the nation's significant potential for renewable energy, particularly in the form of wind and solar resources. The Ethiopian Energy Policy states(6), energy access is crucial for improving the living standards of rural populations, stimulating local economies, and advancing educational and healthcare services. However, much of the rural population remains underserved by centralized energy systems, and this lack of access hampers economic and social development in these areas. Therefore, the need for cost-effective, decentralized energy solutions is more pressing than ever. Small-scale wind turbines (SSWTs) offer a viable solution to this problem, as they can be deployed in remote regions with minimal infrastructure.

The high cost of traditional materials used to make wind turbines is one of the obstacles preventing wind energy from being widely used in rural Ethiopia. Conventional materials, like fiberglass, are costly and have a convoluted supply chain, which makes them inappropriate for small-scale projects, especially in areas with limited resources(7). The challenge lies in finding alternative materials that are not only affordable but also locally available and sustainable. Natural fibers, such as banana fiber, have been proposed as a promising alternative due to their lightweight nature, cost-effectiveness, and environmental sustainability (8). However, research on using banana fiber to create wind turbine blades is still in its infancy, and thorough investigations on their mechanical characteristics, functionality, and suitability for Ethiopian rural electrification programs are lacking.

Another significant issue is the paucity of information and study about the aerodynamic performance of tiny wind turbines made with banana fiber blades. The aerodynamics of the blades play a major role in determining wind turbine efficiency, which impacts the turbine's overall performance and power output(9). There is limited information on how banana fiber blades perform in low-wind-speed conditions, which are typical in many rural regions of Ethiopia. This knowledge gap hinders the development of optimized, high-performance wind turbines that can generate adequate power for off-grid applications. While banana fibers have shown promise in other industries, such as construction and automotive, their application in the wind energy sector remains largely unexplored. Therefore, understanding the aerodynamics of wind turbines using banana fiber blades is crucial for improving their performance in the context of rural electrification in Ethiopia.

The site-specific difficulties in deploying small-scale wind turbines in Ethiopia are another important problem. There is significant regional variation in wind direction and speed, and the nation's wind resources are not consistent. Finding the best places to install wind turbines is essential to guaranteeing the effectiveness of wind power generation, claim Thomas et al. (2018). The viability of employing small-scale turbines for reliable power generation is called into question because wind speeds in rural Ethiopia are frequently below the criteria needed for commercial turbines(10).

Last but not least, consideration must also be given to the socioeconomic environment in which Ethiopia plans to install small wind turbines. High initial investment prices, a lack of maintenance experience, and the availability of turbine system spare parts are some of the challenges that rural electrification projects frequently encounter (15). Small-scale wind turbines may become more inexpensive due to the low cost of banana fiber blades, but the sustainability of these projects ultimately rests on the capacity of local populations to run and maintain the devices. The long-term viability of wind energy projects in rural areas depends on training and capacity-building initiatives, as well as efficient local support systems. In addition, it is essential to ensure that these projects are economically viable and that they contribute to local job creation and sustainable development.

1.3 Objective of The Study

1.3.1 General Objective

This study's main goal is to build and produce a tiny wind turbine for Ethiopian rural electricity using banana fiber as a composite material.

1.3.2. Specific Objectives

The following particular goals will be pursued in order to fulfil the primary goal.

- To design a small-scale wind turbine system that utilizes banana fiber-based blades.
- To investigate the mechanical properties of banana fiber and assess its suitability as a material for wind turbine blades.
- To fabricate and test the small-scale wind turbine model using banana fibers

1.4 Significance and Scope of the study

1.4.1 Significance of the Study

This study is significant in addressing the pressing issue of rural electrification in Ethiopia, where a large portion of the population lacks access to reliable electricity. By designing and manufacturing small-scale wind turbines using banana fiber, a sustainable and locally available material, the research presents a cost-effective and eco-friendly solution for renewable energy generation. The use of banana fiber not only reduces the reliance on expensive imported materials like fiberglass but also promotes local resource utilization and socio-economic development through job creation and sustainable agricultural practices. This innovative approach has the potential to contribute to Ethiopia's energy goals and enhance the quality of life in rural areas.

1.4.2 Scope of the Study

The scope of this study focuses on the design, fabrication, and testing of small-scale wind turbines using banana fiber blades, tailored for rural areas of Ethiopia with moderate wind resources. The research will assess the mechanical and aerodynamic properties of banana fiber for wind turbine blades and evaluate their performance under low-wind conditions typical of rural Ethiopia. It will also explore the feasibility and cost-effectiveness of deploying such turbines at the community level, considering the local economic and environmental context. The study aims to provide a practical, scalable solution for rural electrification and contribute to the broader efforts of sustainable energy development in Sub-Saharan Africa.

CHAPTER TWO

LITERATURE REVIEW

This chapter presents the current state of the art for wind turbines, together with the theory and a brief historical perspective. Section 2.1 covers the basic concept of wind turbines as well as its classification and design. A brief history of wind turbines is given in Section 2.2. Section 2.3 gives the theoretical basis of the several elements that need to be considered while developing the turbine blades. The material often used for the blades, their structure models, cross-sectional area analysis models, aerodynamics, and manufacturing procedures are all covered in this section. The kinds of towers commonly seen in small wind turbines are covered in Section 2.4. Section 2.5 presents the turbine hub concepts for small wind turbines. The turbine nacelle is briefly discussed in Section 2.6. Section 2.7 gives a summary of the many components that comprise the drive train system. Joining and fastening are briefly discussed in Section 2.8. In Section 2.9, the use of wire rope in wind turbines is explained. Section 2.10 describes the type of generator used in wind turbines. A synopsis of the wind turbine-specific control mechanism is given in Section 2.11. Section 2.12 only addresses challenges associated with small wind turbines.

2.1 Basic Concept

An apparatus that converts the kinetic energy of the air into mechanical and electrical energy is called a wind turbine. The turbine blades absorb the air's kinetic energy and convert it into mechanical or electrical energy, depending on the intended use (16–18).

The way wind turbines produce the torque needed to provide the required power determines their classification. When the force is generated by lift force, they are known as lift-type turbines. Turbines that use drag force as a force-producing mechanism are known as drag-type turbines. Furthermore, the rotational axis of wind turbines is used to classify them (19). When the rotating axis is horizontal, they are called horizontal axis wind turbines (HAWT), and when it is vertical, they are called vertical axis wind turbines (VAWT) (20,21).

The vast majority of modern wind turbines are designed using the lift force-based idea. The intrinsic inefficiency of drag-type turbines and the challenge of protecting them from high winds are two of their main problems (22, 23). The HAWT is commonly employed in the business sector because of its great efficiency and relatively low cost per kWh produced. In the 1970s and 1980s, both the US and Canada conducted extensive research into VAWT, with a focus on the Darrieus turbine. They were found to have serious reliability problems and to have energy costs that do not correspond with their horizontal contour section.

The HAWTs can be grouped in a number of ways based on the aspect of interest that one wishes to explore. If the wind orientation is the relevant factor, HWAT are classified as upwind (when the incoming wind passes through the blades before reaching the tower). and downwind, which happens when the wind enters the tower and goes through it before it reaches the blades (24). Depending on how many blades it employs, a HAWT can be called a one, two, three, or more bladed turbine. Because of the hub configuration, the turbine is classified as a stiff or teetering turbine. Depending on the type of control used to adjust the load and power, the turbine is known as a pitched or stalled turbine. The purpose of active yaw turbines, sometimes referred to as passive yaw turbines, is to align with the wind (24). The main pieces of a HAWT are the rotor, hub, drive train, nacelle, tower, foundation, machine control, and electrical system balancing. The HAWT system's schematic is depicted in the figure below.

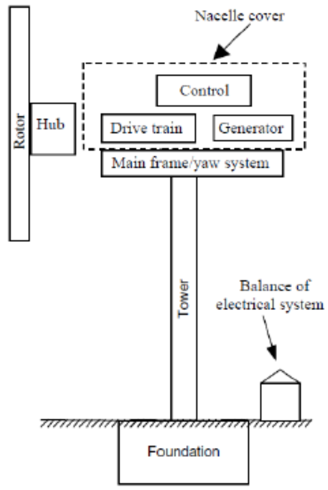

Figure 2.0.1:Wind Turbine Main Parts (24)

2.2 Historical Background

Since the wind was the main energy source for ships and boats in the past, there has been a need to convert wind energy into meaningful activity. Later on, people exploited the wind to power grain mills and water pumps. The first known windmill design dates around 200 B.C. The Persians used windmills to crush grain during this time. The windmills were orientated vertically and were intended to be propelled by drag forces (25). The best materials to employ for the sails were bundles of reeds or wood. A vertical shaft was fastened to the grinding stone, and the sails were joined to horizontal struts that served as the primary shaft. The size of the sails, which were typically 5 m long and installed on a 9 m tall tower, depended on the kind of materials employed in their construction (26,27). Windmills first appeared in Europe in the tenth or eleventh century (28). It rotates on a horizontal axis and were propelled by lift forces. They were employed in almost all mechanical power-intensive operations, including cutting wood, pumping water, grinding grain, and powering equipment. To align the rotor with the incoming wind, the machine's tail was manually adjusted; to protect the windmill, the machine had to be turned away from the wind or the canvas had to be taken off the rotor when the wind speed was high (28).

Before the Industrial Revolution, the primary power source was wind. During the Industrial Revolution, wind energy started to lose ground to thermal energy since it could not be dispatched or transported.

In Denmark, the first wind-powered power plant was constructed in 1890. This contraption served as the model for the modern wind turbine. This apparatus was used to provide energy in isolated locations. During this time, a 17-meter rotor wind turbine electric generator was built in Cleveland, Ohio. With a rated output of 12 kW, the turbine operated for 20 years (29).

A renewed interest in the development of wind turbines for electricity generation was spurred by the oil crisis of 1972. The wind turbine was just a few hundred kilowatts in size until 1992. However, the turbine's size and capacity increased as technology developed. By the end of 2002, we observed a 1000% increase in turbine size (30,31). The largest turbine in operation right now is 164 meters in diameter and has a 10 MW power rating.

Ethiopia is widely recognized for its abundant renewable energy potential, including wind, solar, geothermal, and hydro resources. While national policy frameworks advocate diversifying energy sources beyond dominant hydropower, progress in wind energy – especially small-scale wind – has been comparatively slow(30)

Most research on wind energy in Ethiopia has focused on **r**esource assessment, hybrid system feasibility, and potential energy planning rather than large fleets of installed small wind turbines. For example, studies have explored the feasibility of hybrid PV/wind systems for off-grid rural electrification, indicating the promise of combining wind with solar in remote areas where grid extension is difficult. A specific technical study designed and analyzed a small-scale horizontal-axis wind turbine (~25 kWh output) tailored for household energy use in Addis Ababa, showing SWT technology can be viable at small energy scales. Deutsche Gesellschaft für Internationale Zusammenarbeit (GIZ), through the European-funded Energising Development (EnDev) programme in Ethiopia, works to boost renewable energy markets and access(31). EnDev is focused on *rural electrification, clean cooking, and market development* of technologies like solar PV and clean cookstoves. A project in Jijiga (Somali Region) where a *locally constructed small wind turbine (~3 m rotor diameter)* was installed with solar panels to power a rural shop and provide lighting and productive use load support. This project was implemented by Wind Empowerment, Mercy Corps Ethiopia (through the PRIME programme) with technical support from researchers and local technical college participants (32)

2.3 Turbine Blade

2.3.1 Aerodynamics of Blade Model

The aeroelastic model of a wind turbine is usually created using one of four models: the Blade Element Momentum (BEM), Computational Fluid Dynamics (CFD) model, vortex model, and actuator type model.(11).

Beam Theory

The BEM theory's view of the blades as elements that do not interact aerodynamically is known as "blade element theory." Each of them has distinct airfoil aerodynamic properties. Combining momentum theory and blade element theory yields the blade element momentum (BEM), which makes it possible to calculate the aerodynamic performance characteristics of turbine blades(12,13).

By using empirical modifications generated from wind turbine or helicopter applications, several of the original BEM theory's shortcomings are solved(14–17).

The below discussed issues are the limitation of BEAM Theory.

- **Dynamic Inflow:** It is the response of the flow field to changes in wind turbulence and/or rotor operating conditions. If the inflow changes before the system reaches equilibrium in a new position, there is a temporal delay that depends on the wind speed and rotor diameter (35). This constraint is taken into consideration by the Øye model (41,42), the Pitt-Peters model (39), or the Henriksen model (40).
- **Turbulent wake condition:** The BEM is considered invalid when the axial induction factor is more than 0.4. Several models for corrective action were developed (43). Examples include the GH-Bladed model (41,43,44), AeroDyn Spera model, model, Burton model, Buhl model, and Glauert model (44).

- **Tip loss**: is caused by air moving around the tip of the blade as a result of the pressure differential between the top and bottom surfaces, which reduces lift and eventually causes power loss (45). Usually, the Prandtl correction model is used to account for tip loss. After revising the Prandtl model (48), they were able to obtain results that matched experimental evidence (46–48).
- **Dynamic stall:** refers to abrupt or quick aerodynamic changes that result in stall delays. Numerous models have been created to take the dynamic stall into consideration. The Beddoes-Leishman model(18), Snel model (19), ONERA model(20), Boeing-Vertol model (21), Øye model, and Risø model(22) are included below. None of the models outperforms the others in every way, despite the fact that they all exhibit a strong correlation with the experimental data(22).
- **Stall delay:** is due the rotation of the blades. For models of stall delay, refer to(23,24).
- **Radial flow:** is the flow through the blade's axis; the adjustments model may be found in (25).
- **A skewed wake:** is produced when the rotor axis and the entering airflow form an angle. For the corrective model, see (56). For simplicity and computational convenience, only the first two correction models will be considered in the current study's basic design; CFD studies will be conducted to improve the model in later chapters. BEM takes incredibly little computing time in comparison to other models. If reliable aerodynamic data for the airfoil is provided, BEM produces correct results (57).

Vortex Model Method

Vortex wake methods determine the arrangement of vorticity in the wake region to compute the resulting velocity field (58). The wake is determined by the vortex model using either the free-wake approach or the previously established wake method. The previously described wake approach uses a semi-empirical formulation to characterize the wake from the blades, assuming that it behaves like a rigid body (59). The Free-wake model is used to model unsteady flow. For further information on the application of free-wake in wind turbines, see (60,61).

The vortex model is rarely used in wind turbine simulations due to its higher processing power requirements compared to the BEM model and its tendency to diverge due to the complexity of the changing wake.

Actuator Type Model

The actuator type model is most likely the first model used to examine rotor performance. It manages the scattered loads on the turbine blade as a surface, line, or disc (62). Usually, the actuator disc model is numerically linked with the Euler or Navier-Stokes's equations (62,63).

Because the Navier-Stokes's equations need to be calculated, the actuator disc uses more processing power than the BEM model. The actuator type model assumes that the stresses on the blades are calculated using blade element theory and tables of airfoil aerodynamic characteristics. However, this method is not superior than the BEM model in terms of accurately forecasting the aerodynamic loads (63).

Computational Fluid Dynamic Model

Computational fluid dynamics (CFD) has been widely used in the wind turbine sector due to its ability to produce precise results and efficient flow visualization. In CFD, the governing equations are numerically solved through the use of computer techniques. The wind turbine is governed by Navier-Stokes's equations in conjunction with continuity and energy equations.

It is believed that the wind turbine's flow is incompressible. To simulate a wind turbine using CFD, a 3D CAD model needs to be created using one of the many CAD modelling packages available. To solve the governing equations at a set of predefined points, the CAD model is discretized (meshed) using a mathematical process that converts the governing equations from a differential form into algebraic equations.

To determine any values of the flow parameters across the flow domain, the computed results are interpolated from the predefined locations. After the calculations are finished, the results are post-processed to look at parameters or display the flow.

The three main categories of meshing are structured, unstructured, and hybrid, which combines the two. The advantages of structured mesh include fast convergence, low memory needs, and high resolution. The unstructured mesh usually generates more cells than the structured mesh. This fact increases the computational time needed to converge to a solution when using an unstructured mesh in CFD. Hybrid mesh, sometimes referred to as adaptive mesh, combines the two mesh types. This mesh gives you the option to employ unstructured mesh in areas with intricate shapes and structured mesh where appropriate. This mesh has been widely used in wind turbine CFD simulations (64).

The three most popular techniques for discretizing the governing equations used in CFD are the finite volume method (FVM), finite element method (FEM), and finite difference method (FDM). Most CFD models use FVM since it takes up less area, which means it uses less memory and processing time. FEM can be used in CFD modelling even though it is frequently used in structural analysis. Despite being significantly more stable than FVM, FEM requires more memory for computational space, which causes it to compute results more slowly. Despite being simpler to use than the other three methods, FDM is only used in simple applications (65).

Turbulence models must be created in order to use the Navier-Stokes's equation to solve wind turbine difficulties. Models such as the ω-k SST model (67), which is based on the Reynold Averaged Navier-Stokes turbulence model, and the Spalart-Allmaras model (66)[51,21] have been employed for wind turbine applications. When modelling two-dimensional airfoils and three-dimensional blades in CFD, the omega-k SST model is preferred over alternative methods (68).

2.3.2 Blade structure Model

To fully develop an elastoplastic model for a wind turbine blade, it is necessary to comprehend the structural blade's reaction. Two models the three-dimensional finite element method (3D FEM) model and the one-dimensional equivalent beam model describe the structural reaction of the blade(26). Using the 3D FEM model with the commercial FEA requires a significant amount of time and work. However, because it yields accurate results when paired with CFD, it has been used to develop the aeroelastic model for wind turbine blades (69). Since a typical wind turbine blade has one dimension that is much larger than the other two, it may be modelled as a one-directional beam with a span along the longest dimension and a cross-sectional area perpendicular to it. Therefore, beam model theory can be used to investigate the structural response of wind blades.

There are two types of beam theory: linear and nonlinear. The Euler-Bernoulli beam model and the Timoshenko beam model are the two most widely used models in beam theory. When applied to wind turbine blades, these models produce results that are comparatively similar. Due to its ease of usage, the Euler-Bernoulli model is increasingly frequently used in the structural modelling of wind turbine blades. When a nonlinear wind turbine blade model is needed, the Nonlinear Aeroelastic Model for Wind Turbine Blades (NAM_WTB) is used because it offers an excellent approximation with experimental results. The modal methodology, one-dimensional finite element method (FEM), and multi-body dynamics (MBD) are used to discretise wind turbine blades. Recent developers have created models of aeroelastic wind turbine blades using the one-dimensional FEM(27,28).

2.3.3 Blade cross-sectional analysis model

The cross-sectional properties of wind turbine blades can be ascertained using one of three models: the two-dimensional FEM-based model, the three-dimensional FEM-based model, or the classical lamination theory (CLT)-based model. Every model has some shortcomings(29).

Classical lamination theory's (CLT) precision and efficiency are commendable. It has been widely used to investigate the structural response of the composite material. Of the three models used to determine the cross-section of the blade, CLT is the most efficient. However, because shear deformation is not taken into consideration while evaluating the cross-sectional properties, it is not suitable for use with short and thick blades(30).

The 3D blade model is converted into a two-dimensional model using the two-dimensional FEM-based model using a pre-processor. The two-dimensional FEM-based model requires less processing power than the 3D FEM-based model. However, because they needed a preprocessor, they were less efficient.(31).

Of the three, the 3D model-based model is the most intricate. Although it provides precise stress analysis and displacement, it does not consistently produce the cross-sectional property of wind turbine blades(31).

STALLVIB, ADAMS/WT FAST, FLEX5, GAST, GH-Bladed, HAWC2, and PHATAS are the most widely used aeroelastic models in the wind turbine industry.

2.3.4 Material for Wind Turbine Blade

The wooden blades of early wind turbines were sometimes folded with cloth. Later, in the 1950s or so, turbine blades were made of metals, especially steel. Since the 1970s, most horizontal axis wind turbine blades have been made of composite materials. Fiberglass in polyester resin is the most widely used blade material, but vinyl ester and wood epoxy laminates have also been used.(32).

Materials used in wind turbine blade design should have long life cycles, high stiffness, and a high strength to weight ratio. Additionally, the material should be affordable and easily available, and the related manufacturing processes should be economically priced. Wood, metals, polymers, and composite materials have all been used in the creation of wind turbine blades.

Wood: Because wood is environmentally benign, it is a very attractive material for wind turbine blades. Their strength to weight ratio is comparatively high. They also have good fatigue strength if they are properly aligned. However, wood is prone to dampness and is not widely available with a consistent quality. It can be expensive to mold wood into intricate blades. Consequently, wood is only used in small wind turbine applications where the blade diameter is less than 2.5 m (32)

Metals: Steel is used extensively in many engineering applications. In the past, it was used to make wind turbine blades instead of wood. Steel has a high density. This information was used to stabilize the turbine's output power because steel is relatively less expensive and the mass moment of inertia rises with blade weight. However, due to its low strength to weight ratio, poor machinability, and low fatigue strength, steel is no longer used to make wind turbine blades. Aluminum is the most common metal on Earth. It offers a greater strength to weight ratio, is substantially lighter than steel, and is relatively cheap. However, steel is more fatigue-resistant than aluminum. Currently, tiny wind turbines with consistent blade cross-sectional areas and wind turbine tests are designed using aluminum.

Composite Materials: Composites are the most often used materials for wind turbine blades. They feature a high stiffness to weight ratio, high strength, good fatigue strength, and resistance to corrosion and environmental deterioration. They can also be readily molded into complex shapes using a range of methods. To make a composite material, two distinct materials mostly fibers are held together by a binder matrix. Composites are composed of fiberglass, carbon fibers, and wood. They are bound with polyester, epoxy, or vinyl ester. The most widely used composite material for wind turbine blades is glass reinforced plastic.

Fiberglass: The two forms of fiberglass that are most frequently used in wind turbine applications are S-glass and E-glass. S-glass has a 25–30% better tensile strength than E-glass, despite the fact that E-glass is about twice as expensive. Tows, also known as unidirectional bundles of fibres, are used when exceptional strength is required.

Binder: The benefits of epoxies include their superior adhesion, reduced shrinkage after curing, and exceptional chemical resistance. They are also more active. Nevertheless, they cost roughly 1.5 times as much as polyesters, and polyester takes less time to cure. Epoxies-based resin and vinyl esters are comparable, but vinyl esters are less expensive and require less time to cure. Additionally, they are more stable in the environment.

Carbon Fiber: Although carbon fiber is more durable than fiberglass, it costs about eight times as much as fiberglass (33). Instead of replacing glass in wind turbine blade construction, carbon fiber is utilized in conjunction with glass to reinforce the materials at the blade's specific spot where it is required.

Laminated Wood: Wood has an exceptional strength to weight ratio and good fatigue strength. Wood is occasionally chosen over synthetic fibers for composite products. Douglas Fir is the most widely used wood in wind turbine applications.(34). Wood-epoxy laminates exhibit favorable fatigue properties. Wood epoxy turbine blades have never experienced fatigue-related failures in operation.

2.3.5 Blade Manufacturing Process

There are variety of methods that can be used for manufacturing of Wind turbine blades. The material, size, and shape of the blade determine the method to be used; financial limitations are also crucial.

Wood Technology: In cases when wood is the preferred material for the turbine blade, the techniques used are hand carving, a copying machine, or a computer numerically controlled (CNC) router. Even though CNC routers are incredibly accurate and durable, it can be expensive to use them to make turbine blades, particularly if the blades are small. Despite being less costly than CNCs, it was found that it was inappropriate to convert a commercial equipment designed for gun stocks and other comparable items to the production of blades, especially for blades with a tip chord of about 5 cm. Despite being less costly, hand carving produces blades with subpar performance(35).

Hand -Lay -Up: The technique known as "hand-lay-up" involves manually laying fibers or other reinforcing materials on the mold and infusing them with resin. Squeegees or rollers are used to force the resin into the hole. Although this procedure is straightforward, it requires a lot of work. Because the worker determines the product's quality, it is challenging to consistently produce high-quality products. This procedure also has the disadvantage of releasing fume into the room, which puts the workers at risk of breathing it in(36).

Pre- Preg: The pre-preg technique involves placing the impregnated glass on the mould and applying heat to allow the resin to flow and solidify the substance. An autoclave or a low-temperature oven are used for the heating process. Resin to fiber consistency may be achieved using this process, and satisfactory outcomes are easily produced. However, the material may cost more.

Resin Infusion: After the dried reinforcing material is put into the mould, a carefully engineered mechanism presses resin into it. In one type of infusion technique known as vacuum-assisted resin transfer moulding (VARTM), air is removed from one side of the mould using a vacuum pump. A hoover bag is placed over the mould to create a vacuum. The hoover bag allows the resin to flow from an external reservoir to the mould. The exterior reservoir is accessible to the atmosphere. Compared to the hand-lay-up process, resin infusion yields a higher-quality end result and doesn't release any fumes into the surrounding area. (36).

Pultrusion: By pushing material through a die, the manufacturing process known as pultrusion produces an object with a predefined cross-sectional area. Pultrusion is the preferred method when producing vast amounts of homogeneous cross-sectional area(34).

Filament winding: The process of filament winding involves simultaneously placing the resin and winding the fiberglass around a mandrel. This technique is widely employed in wind turbines and the aerospace sector. The concave surface is not suitable for filament winding(37–40) .

2.4 Other components of wind turbine

Tower: of order to place the nacelle and rotor at the proper height, the tower of a wind turbine system must transport all component loads to the foundation. For a turbine to operate effectively, the tower needs to be somewhat stable and structurally strong, and vibration needs to be considered as well. The main tower types used in modern turbines include guyed towers, lattice towers, and tubular steel towers(41–43).Lattice towers use roughly half as much material as tubular towers for the same height. They therefore require a lighter foundation(43). Lattice towers' primary drawbacks are its low aesthetic appeal, increased bird activity, and maintenance challenges. The tubular tower provides the best bending resistance in all directions due to its round cross-section. These towers greatly reduce avian activity, provide a safe climbing area for maintenance, and are aesthetically pleasing(42).

A tower with guyed steel poles can hold a small wind turbine. This method is less expensive because it allows for the construction of a much lighter tower than would have been necessary otherwise because the tower and the guy wires share the load. Four cables that are equally spaced and orientated at a 45-degree angle usually support the tower (85,86).A tower is usually at least 20 meters high. For large wind turbines, they ought to be one to one and a half times the rotor diameter(41).Over the course of its lifetime, the wind turbine tower is subjected to two major types of wind load: steady and dynamic. When constructing a wind turbine tower, it is necessary to consider at least two load scenarios: operating at the rated power and the stationary survival wind speed. The International Electrotechnical Commission's (IEC) recommendations for surviving wind speed recommend a 50-year extreme wind speed(43).The rotor may cause the tower to vibrate. The stability of the tower must be carefully considered since it affects the dynamic system response to the rotor excitation. The tower's inherent frequency shouldn't coincide with the rotor or blade-passing frequencies(43).A wind turbine tower's structure can be studied using the Finite Element Method (FEM) or the classical theory of beams. Wind turbine towers are usually made of steel that has been coated to prevent corrosion. Sometimes concrete is used as well.

Hub: Attaching the blades to the main shaft is the hub's function in a wind turbine. The blades are responsible for carrying and transmitting all of the loads they create. Hubs are usually made of steel, either by welding or casting. There are three types of hubs: hinged blade hubs, teetering hubs, and rigid hubs(44).When the pitching of the blade is the only relative movement allowed between the hub and the main shaft, the hub is said to be stiff. Rigid blades are used in turbines with three or more blades. The parts that attach to the main shaft and those that connect to the blades move relative to one another in teetering hubs. In this gadget, the blades rotate up wise. Usually, wind turbines with one or two blades employ teetering hubs. At the moment, no commercial wind turbine uses a teetering hub(45).

Nacelle: Every part of the turbine is housed in the nacelle. It protects the parts that are susceptible to environmental changes. The generator, gearbox, driving train, and control systems are installed there. The mainframe and the nacelle cover make up the nacelle.The mainframe serves as both a point of attachment for the yaw bearing and a source of rigidity, which keeps the parts aligned and prevents them from moving in relation to one another when the system is operating. The mainframe sends loads to the tower from the rotor, generator, gearbox, and tail. There are two types of frames: a gearbox mainframe and a separate mainframe. The independent mainframe is a rigid steel casting or weldment with the appropriate holes and other attachments for attaching the parts. The gearbox mainframe is made to be strong enough to sustain all necessary loads and features holes and other connection points to enable the assembly of other pieces. Rain, moisture, ice, snow, sunshine, salt, and solid particles (airborne grains) are all shielded from the turbine and control system by the nacelle cover. Noise-reducing materials can be added to the nacelle cover as necessary. Air can flow through the components of the nacelle thanks to its design. Where necessary, this design strategy makes it easier for the components to cool. Because fiberglass has a high strength-to-weight ratio, it is typically used for nacelle covers. The nacelle house on small and medium-sized turbines is often built to make the components easily accessible when it is opened (46)Drive Chain The main machine components of a wind turbine are its shaft, bearings, coupling, brakes, gearboxes, clutches, dumper, springs, attaching and joining, and wire rope. These parts are commercially available and manufactured in compliance with current engineering requirements.

The design of those components is the subject of numerous literary works. The design of machine elements is covered in great detail in any machine design textbook. Below is a brief discussion of each element component as it relates to wind turbine design.

Main shaft: The main shaft of a wind turbine transfers the rotational power from the generator's blades. The primary shaft is subjected to both a torsional load and a bending moment. The shaft needs to be constructed with fatigue in mind because the loads usually fluctuate over time. The shaft should not operate at critical speeds close to its inherent resonance frequencies in order to avoid significant vibrations. Bearings on the main shaft sustain the loads on the rotor blades, transferring the stress to the mainframe. Keys are used to secure the shaft to the hub of a tiny wind turbine. Additional techniques for attaching the shaft to the hub include the Ring Feder Shrink Disc and a permanent angle that is fastened to one end of the shaft and bolted to the hub (46). The kind of material to be used depends on the main shaft's operating circumstances. When the operating circumstances are less severe, hot-rolled plain carbon steel is usually used. Steel is typically strengthened by adding more carbon if the application calls for more strength. Alloy steel is used in demanding operational settings. The shaft is frequently heat-treated after machining to increase its hardness and yield strength. (46).

Bearings: provide relative motion, usually rotational motion, between surfaces. In wind turbines, bearings are used in the generator, yaw mechanism, pitch control, gearboxes, primary shaft, and some teetering systems. Ball bearings are the most often used bearing type in wind turbine design. They are typically made of steel. Wind turbine gears also make use of roller bearings.

Important considerations while designing the bearings are the load they will experience and the expected number of cycles(46).

Couplings: are mechanical components used to transfer torque between two shafts. The connection connects the generator to the gearbox or main shaft in a wind turbine. They are made composed of two sections joined by bolts (reliable coupling); often, a key is used to stop the pieces from rotating against the shafts (46).

Gear: Wind turbine parts called gears move energy from the rotor to the generator at a variable rotational speed. Wind turbine gear is made of steel that has been heat-treated to produce high strength and surface hardness. Wind turbines need a gearbox because their blades move more slowly than those of traditional electrical generators (60 or 50 Hz). Because the load conditions found in wind turbines differ greatly from those seen in other applications, the gears used in wind turbines are distinct. It is said that poorly constructed gearboxes are the root cause of many wind turbine operational problems. The gearbox is one of the largest and most expensive components of a wind turbine(46).

Clutches: are components that isolate a system component from torque while they are disengaged and transfer torque to that component when they are engaged. Pitch linkage and clutch-type brakes in wind turbines both require clutches. Clutches are engaged by springs and disengaged by a mechanical or electromechanical system(45,46).

Brakes: Both mechanical and aerodynamic brakes are commonly found in wind turbines. Stall is regulated by aerodynamic brakes, which are controlled surfaces on the blade. flaps, can spoilers, tip brakes, or aerodynamic brakes. Surfaces can enter and exit the blade as needed thanks to electromagnets that control the aerodynamic brakes. In addition to stopping the turbine and carrying out maintenance duties like parking brakes, the mechanical brakes act as a backup system for the aerodynamic brakes. They are also a part of the systems that control pitch and/or yaw. Clutch and disc brakes are the two most popular mechanical brakes found in wind turbines. Disc brakes are operated by a hydraulic system, whereas clutch brakes are operated by spring and pneumatic or hydraulic systems.

Anywhere along a wind turbine's drive system, brakes can be installed. When fitted on the low rotation side, the brakes need to provide greater torque than when placed on the high rotation side. Consequently, a heavier and more power-hungry brake system will have to be constructed. However, putting the brakes on the side with the highest rotation may wear down the gearbox, and the brake might not be able to stop the rotor if the gearbox breaks.(46).

Springs: are used in passively actuated safety systems in wind turbines, including the rubber damper, teeter damper, aerodynamic surface, brakes, and blade pitch linkage. Typically, springs are made for torsion, compression, or tension purposes. Steel wires formed into spiral coils are used to make the most popular springs (46).

Dampers: Wind turbines use dampers to reduce the adverse effects of dynamic loads. The three main kinds of devices used as dampers in wind turbines are hydraulic pumping circuits, fluid couplings, and linear viscous fluid. Fluid couplings are used to reduce torque variations. In rotors with one or two blades, linear viscous fluid dampers are employed as a teetering damper. Hydraulic pumping circuits are used when yaw motion dampening is necessary(45,46).

Fasteners: are used to attach components in a way that makes it simple to remove them when needed. Bolts and screws are the most common fasteners. Fatigue is the primary factor that needs to be considered when designing the fastener, and it can be minimized by pre-stressing the bolts. The vibrations and shocks that wind turbines experience can cause bolts and screws to come away. Various methods are employed to tackle this problem, including washers, lock nuts, lock wire, and chemical locking agents. Welding, riveting, soldering, and adhesive bonding are some of the methods used in wind turbine design to link components that are difficult to remove (45,46).

Wire rope: is typically used in guyed wind turbine towers or meteorological masts to stabilize the tower. When the turbine is being built, the wire ropes are also used. Tensile strength is the most important consideration when building a wire rope. Fatigue is another important aspect. When lifting, sheaves or pulleys are sometimes used to prevent the wire rope from suddenly changing direction. The sheave must have at least 20 to 40 times the wire rope's diameter.(45,46).

Generator : The most common types of generators found in wind turbines are synchronous, DC, induction (asynchronous), and permanent magnet synchronous generators (PMSG) for modest applications. In certain cases, direct-drive generators are also considered (89).

Power electronic converters in variable-speed wind turbines and large grid-connected wind turbines are examples of wind turbines that occasionally use synchronous generators.

Permanent magnet synchronous generators are used in some independent wind turbines. Before being supplied to the desired use, the output power is often converted into DC (46).

An induction generator is used by wind turbines most of the time. Their simplicity, durability, affordability, and ease of connecting and disconnecting from the grid are their advantages (46). Smaller, battery-charging wind turbines were often powered by DC generators. However, DC generators are rarely used in wind turbine applications these days due to its high cost and maintenance(46).

Permanent magnet generators are recommended for small wind turbine applications with a minimum power of 10kW. Large wind turbine applications also make use of permanent magnet generators. The generator's stationary armature serves as the source of electricity. As a result, commutators, brushes, or slip rings are not necessary. The permanent magnet generator is highly robust due to its straightforward design (46).

Permanent magnet synchronous generators (PMSG) are another term for permanent magnet generators. The production of magnet fields is the main way that they differ from synchronous generators. The synchronous generator uses an electromagnet, while PGSM uses a permanent magnet. One particular type of synchronous generator is a direct drive generator. Without the need for a gearbox, these generators are constructed with enough poles to allow the wind turbine rotor to be connected directly to the generator. However, because there are so many poles, the generator's diameter must be fairly enormous.

A control system: is necessary for wind turbine applications in order to maximize power generation, ensure the turbine's safe operation, reduce operating costs, and minimize induced loads. Controlling a wind turbine involves pointing it in the direction of the wind, preventing it from moving too fast, and monitoring the quality of the electricity it generates for the final consumer. The dynamics control level and the supervisory control level are the two control levels in wind turbines that need to be considered.The supervisory control keeps an eye on and manages both the turbine operation and the order of control actions. Dynamic control regulates the turbine's reaction to environmental changes that may impact its integrity or performance(46).Monitoring for safe operation, collecting and reporting data, managing turbine operation, and triggering safety and emergency systems are all part of the supervisory control's duties(46).In wind turbines with generators running at constant speed, torque can only be controlled by adjusting the aerodynamic torque. Either the generator torque or the aerodynamic torque can be changed to adjust torque in variable speed generator turbines.To adjust the aerodynamic torque, the blade surface is changed using pitch control, ailerons, spoilers, and patchable tips.

2.5 Small scale wind Turbine

Since the 1970s, small wind turbines have advanced considerably. However, this technology still has reliability and turbine noise problems. Therefore, more study is needed to ensure that small wind turbines operate reliably and to reduce noise levels to tolerable levels(46).

Government subsidies are essential to the profitability of small wind turbines (SWTs), as many SWTs are not economically viable. A model based on the turbine Air X was presented by Sleiti and Mehrabian (47), who altered the nacelle, generator, tower, yaw system, and rotor design. It was discovered that an average household using this approach would save about $137 annually. Design, dependability, and simplicity are more cost-effective for tiny wind turbines than state-of-the-art technology. A turbine that cost as little as $1000 per kW was reported(47).

De Freitas et al. state that in order to optimize a turbine's aerodynamic blades, the drag to lift ratio ought to be as low as practical. Shen looked studied how to optimize small wind turbine blades with three-dimensional blade forms for a number of purposes.(48).

FX 63-137, S822, S834, SD2030, SG6043, and SH3055 are the most often used airfoils for small wind turbines; their thin counterparts offer a higher lift to drag ratio and reduce noise.(48).

A strategy for choosing materials for wind turbine blade design was presented. A computer model can be used to predict the mechanical properties of the fiberglass blade(48).

A model has been created to show that in order to shorten the starting time at low speed while preserving efficiency, the moment of inertia should be decreased by hollowing out the blade(48).

Most tiny wind turbines are installed on steel monopole towers, which are often difficult to transport to a distant location. For a 12 m 500 W turbine, bamboo is a feasible material because, according to Clifton and Wood, the cost of producing a monopole tower can make up 30–40% of the installation cost. They presented numerical optimization methods for self-supporting octal monopole towers. Wood looked into the height that maximizes the turbine's average power production to total capital cost ratio. (49).

Controlling a tiny wind turbine involves pointing it in the direction of the wind, guarding against overspeed, and directing the generator's output toward the desired outcome. In tiny wind turbines, furling is primarily used for power and overspeed control. Audierne et al. presented a consistent Lagrangian formalism-based model of the dynamics of gravity-controlled furling devices(48).

Small wind turbines frequently use permanent magnets to supply the excitation field for the generator. For low-cost rural electricity, the basic theoretical concepts and construction methods of coreless axial flux permanent magnet generators were described in depth(48).

Research gap

Despite extensive research on small-scale wind turbines for decentralized energy systems, most blade designs continue to rely on synthetic composites such as glass fiber-reinforced polymers, which increase production cost, embodied energy, and end-of-life disposal challenges(50). Although natural fiber composites have been investigated for general structural applications, their integration into aerodynamically optimized wind turbine blades particularly using banana fiber (Enset) within rural African contexts remains insufficiently explored in terms of coupled aerodynamic structural optimization, stress validation, and scalable manufacturing(50) Furthermore, limited studies combine blade geometry optimization (chord and twist distribution), finite element stress analysis, and additive manufacturing–assisted mold fabrication within a unified framework targeted at rural electrification. This research addresses these gaps by optimizing blade geometry using SolidWorks simulation to evaluate maximum stress at the root and displacement at the tip, fabricating the blade through digital modeling and 3D-printed mold development, and validating the structural feasibility of banana fiber (Enset) composites. The study contributes a sustainable, low-cost, locally sourced blade design framework tailored for rural electrification, advancing eco-friendly composite utilization and practical small-scale wind deployment.

Table 2.1:- Research gap summary

No	Author(s) & Year	Title	Methodology	Key Findings	Research Gap
1	Amzil et al., 2025	Sustainable Blade Design Review	Critical review & structural analysis	Natural fibers promising for sustainability	No Enset fiber blade fabrication study
2	Samuel et al., 2022	Natural Fiber Polymer Composites for Wind Blade	Literature review	Natural fibers reduce cost & weight	No aerodynamic validation for small turbines
3	Ramli et al., 2018	Natural Fiber Reinforced Composites	Mechanical testing	Banana fiber good tensile-to-weight ratio	No blade structural load case analysis
4	Miliket et al., 2022	Hybrid Natural Fiber Composite Blade	Experimental tensile & flexural tests	Hybrid improves strength	No rural electrification focus
5	Park, 2016	Flax Composite Small Blade Design	FEA structural analysis	Flax viable for small blades	No Enset fiber investigation
6	Varun et al., 2024	Composite Blade Material Evaluation	FEA comparison (GFRP/CFRP)	Synthetic composites high strength	No biodegradable local material study
7	Carnicero et al., 2025	Thermoplastic Blade Manufacturing	Manufacturing + lab testing	Thermoplastic blades feasible	High cost; not rural-focused

No	Author(s) & Year	Title	Methodology	Key Findings	Research Gap
8	Pender et al., 2024	Natural Fibre Feasibility Study	Environmental & structural assessment	Eco-beneficial materials	No full aerodynamic modeling
9	Andoh et al., 2023	Bamboo Composite Blade Fabrication	Fabrication + field test	Bamboo blade possible	No detailed load case validation
10	Chen et al., 2011	Textile Composite Adaptive Blade	Structural optimization	Adaptive blade controls power	No banana/Enset fiber use
11	Khalil et al., 2015	Banana Fiber Composite Properties	Mechanical & microstructure tests	Eco-friendly moderate strength	No wind blade aerodynamic study
12	Dunisho et al., 2020	Enset Fiber Polyester Composite	Impact & absorption tests	Improved impact strength	No turbine blade application
13	MDPI, 2024	Enset–Sisal Hybrid Composite	Mechanical characterization	Hybrid improves tensile strength	No blade validation
14	Scientific Reports, 2025	Alkalization of False Banana Fiber	Chemical treatment study	Treatment enhances strength	No wind energy structural modeling
15	PMC Review, 2017	Materials for Wind Turbine Blades	Comprehensive review	GFRP dominant material	No biodegradable rural solution focus
16	TEAM Project, 2021	Natural Fiber Blade Optimization	Aerodynamic optimization	Natural fiber usable in small turbines	No Enset fiber analysis
17	Oyedepo et al., 2012	Small Wind Turbine Rural Electrification	Performance testing (low wind)	Small turbines viable for rural use	No blade material innovation
18	Ragheb & Ragheb,	Wind Turbine	Material review	Synthetic	No African local

No	Author(s) & Year	Title	Methodology	Key Findings	Research Gap
	2011	Blade Materials		composites dominate	fiber integration
19	Mathew, 2006	Wind Energy Fundamentals	BEM theory foundation	Blade design theory established	No composite material study
20	Tang et al., 2010	Natural Fiber Structural Applications	Composite mechanical analysis	Suitable for structural use	No wind turbine validation

CHAPTER THREE

3. DESIGN AND ANALYSIS

In this chapter, the design and analysis of the Wind energy system will be discussed. The first part of section 3.1 will focus on the blade design and analysis techniques while the under that section 3.1.1will discuss about the determination of blade acronymic analysis. Later at the section 3.1.2 will be discussed about the structural analysis of the wind turbine blade to ensure that the blade is suitable and can with stand the load with different cases of the wind turbine must with stand. At the end of the chapter the 3.1.3 the solid work structural optimization of the blade and how the optimization curried will discussed.

3.1 Methodology

3.1.1 Blade Design

The design of horizontal axis wind turbines begins with aerodynamic study to ascertain the basic dimensions of the blade, including its radius, chord distribution, and twist angle distribution. At this point, the aero foil selection is likewise complete, and the blade's structural design follows. Prior to starting the force and stress analysis, the system criteria, such as cheap cost, strength, and light weight, must be taken into consideration while choosing the materials. The blades must be inspected for the many loading scenarios that they are exposed to during operation and travel in order to determine whether the factor of safety for each load case is more than the safe limit.

The analysis of blade stability, which takes into account buckling, deflection, and vibration, will finish the blade design. Section 3.2 will address the blade's aerodynamic design based on this design flow. The blade design process is based on the flow diagram that can be seen at Figure 3

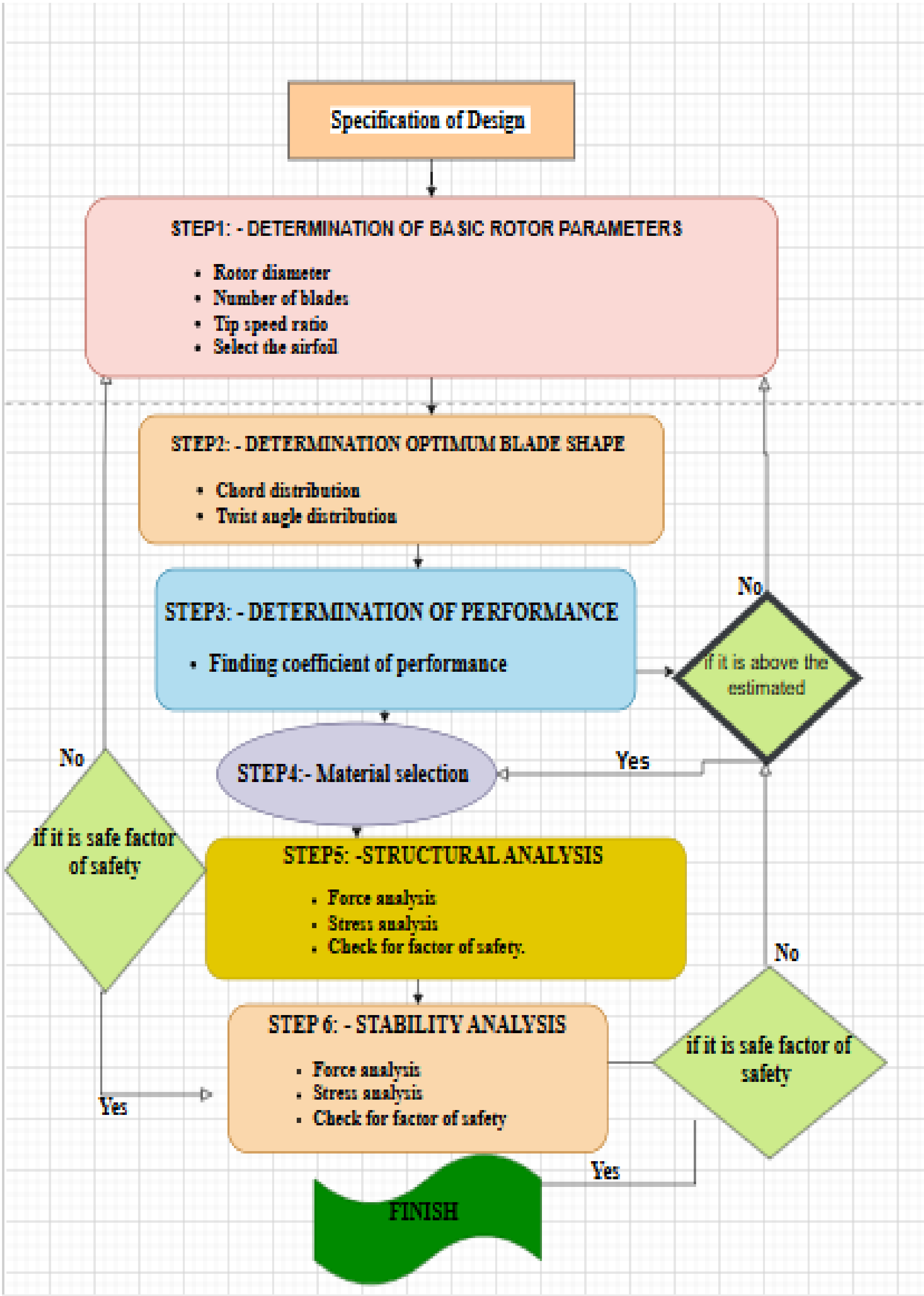

Figure 3.0.1: - Design flow Diagram

3.2 Aerodynamics Analysis

Wind turbine blades are analyzed using a variety of design theories, such as blade element theory, momentum theory, blade element momentum, and others. The analytical design of this thesis work is based on the generalized rotor design approach for the ideal blade form of a rotor with wake rotation, as stated in (5). The effect of the tip loss factor is introduced to account for the loss resulting from the phenomenon that air tends to flow around the tip from the lower to upper surface when the pressure on the suction side of the blade is lower than on the pressure side, lowering lift and, accordingly, power production at the tip.

The tip loss factor can be estimated using a variety of techniques; in this thesis, Prandtl's method, as outlined in [5], is employed. During the actual operation of the wind turbine rotor, the flow behind it rotates in the opposite direction of the rotor in response to the torque that the flow applies to it. The rotor extracts less energy than would be expected without wake rotation due to the generation of kinetic energy without wake, which makes it evident that slow-running wind turbines (those with high torque and low rotational speed) experience greater wake rotation losses than high-speed wind machines with low torque. The design study for this work was predicated on the following assumptions:

- ✓ The Tip loss effect,
- ✓ The blades Finite number,
- ✓ The non-Zero drag force coefficient.
- ✓ There is wake rotation behind the rotor,

Strip Theory for a Generalized Rotor with Wake Rotation

As stated in the paragraphs above, the blade design study is predicated on BEM theory, which takes into account wake rotation, tip losses, and other such elements. The performance of a wind turbine produced by this method is not far from the actual value that is expected. The analysis is based on the four equations from the theories of momentum and blade elements. Additionally, it is expected that the blade's chord and twist distributions are known. Even when the angle of attack is unknown, other relationships can be used to determine the angle of attack and blade performance.

Momentum Theory

From axial momentum and angular momentum(28)

$$dT = \rho V1 [4a (1 - a)\pi rd \tag{3.1}$$

$$dQ = 4a (1 – a) \rho V_1 \pi r^3 dr \tag{3.2}$$

Blade element theory

From blade element theory:

$$dF_N = B \times 1 /2 \times \rho \times V^2{}_{rel} \times (C_L sin\beta + C_D cos\beta)\ cdr \tag{3.3}$$

$$dQ = B \times 1 /2 \times \rho \times V^2{}_{rel} (C_L sin\beta - C_D c\ )\ c \times rdr \tag{3.4}$$

When the thrust, dT, is equal to the normal force, dFN, the differential forces are defined as follows using a sequence of algebraic manipulations.

$$dF_N = \boldsymbol{\sigma}'\pi\rho \frac{V1(1-a)2}{\cos 2(\beta)} * \ (C_L sin\beta + C_D cos\beta)\ rdr \tag{3.5}$$

$$dF_N = \boldsymbol{\sigma}'\pi\rho \frac{V1(1-a)2}{\cos 2(\beta)} * \ (C_L cos\beta - C_D sin\beta)\ r2dr \tag{3.6}$$

Where: $\boldsymbol{\sigma}'$ is the local solidity and defined as;

$$\sigma' = Bc/ 2\pi r \tag{3.7}$$

Blade element momentum theory

It is standard procedure to set the drag coefficient to zero when calculating the induction factor, $and\ a\ '$; this simplification introduces very little inaccuracy. Therefore, combining the torque equation from momentum and blade element theory will provide us with

$$\frac{a}{1-a} = \frac{\sigma'(CLsin\beta + CDcos\beta)}{4Qcos2(\beta)} \quad (3.8)$$

Based on the geometrical considerations we know, blade element theory,

$$tan\varphi = V(1 - a) /\Omega r(1 + a') = V(1 - a) /\lambda r (1 + a') \quad (3.9)$$

Equations only offer a preliminary estimate. The following are the equations.:

$$\beta = 90^o - 2 /3 * tan^{-1} (1/ \lambda r) \quad (3.10)$$

$$a = (1 + \frac{4 \cos 2\beta}{\sigma' CLsin\beta})^{-1} \quad (3.11)$$

And equations 3.9 and 3.10 the following results are developed,

$$Cl = 4 \times sin\varphi \frac{cos\varphi - \lambda r sin\varphi}{\sigma'(sin\varphi + \lambda r cos\varphi)} \quad (3.12)$$

$$a'/ (1 + a') = \sigma' \times Cl / 4cos\varphi \quad (3.13)$$

$$\frac{a'}{a} = \frac{\lambda r}{tan\varphi} \quad (3.14)$$

$$\frac{a'}{a} = \frac{\lambda r}{tan\varphi} \quad (3.15)$$

$$a = \frac{1}{[1 + \frac{4 \times sin\,2\varphi}{\sigma' \times Cl \times cos\varphi)}(\,]} \quad (3.16)$$

$$\acute{a} = \frac{1}{[(\frac{4 \times cos\varphi}{(\sigma' \times Cl)\,)}) - 1]} \quad (3.17)$$

There are two fundamental ways to solve the aforementioned equations and ascertain the forces and flow conditions at each blade segment.

For a given blade shape and operating conditions, method 1 involves solving for Cl and α since θ = α + θp. This leaves equation 3.13 with two unknowns, namely Cl and φ at each section. The empirical Cl Vs α curves for the selected aerofoil can be used to get these values. Equation 3.13 can then be satisfied by determining Cl and α from the empirical data. Both numerical and graphical methods can be used for this [5].

technique 2: iterative solution for "a" and "a '" This technique begins with a and a ′ guesses, from which fresh induction factors and flow conditions are computed.

1. Guess values of a and a ′,

2. The angle of the relative wind Calculation the from equation 3.10,

3. The angle of attack calculation from θ = α + θp and then Cl and Cd.

4. From equation 3.16 and 3.17 Update a and a ′.

This procedure will keep going until the computed induction factors fall within the previously specified tolerance, which is less than a 1% discrepancy.

Calculation of power coefficient

After obtaining "a" from each segment, the overall rotor power coefficient can be computed using the equation given in [5], which was first proposed by Wilson and Lissaman. 1974.

$$C_P = (\frac{8}{\lambda^2}) \int_{\lambda h}^{\lambda} \lambda r^3 \times a'(1 - a)[1 - \frac{Cd}{Cl} cot\varphi] d\lambda r \quad (3.18)$$

Where: λ□= is the local speed ratio at the hub, or equivalently.

$$CP = (\frac{8}{\lambda^2}) \int_{\lambda h}^{\lambda} sin^2\varphi\,(cos\varphi - \lambda_r sin\varphi)(sin\varphi + \lambda_r cos\varphi)[1 - \frac{Cd}{Cl}) \times cot\varphi]\lambda^2 d\lambda r \quad (3.19)$$

Tip Loss: Effect on Power Coefficient of Number of Blades

When wind turbine blades are operating, air tends to flow around the tip from the lower to upper surface because the pressure on the blade's side is slower than on the pressure side. These lowers lift and, consequently, power output close to the tip. Several approaches have been proposed to incorporate the tip loss effect. The model created by L. Prandtl is the most suggested among such techniques for the reasons listed below.

- The predictions of the Prandtl model qualitatively match the HAWT rotor behavior.
- The Prandtl model's calculations of rotor power and thrust accord well with test results.
- The results of BEM theory calculations using the Prandtl model and vortex theory calculations accord well.
- The Prandtl model is simpler to use and program. According to this method, a correction factor, F, must be introduced in to the previously discussed equations. This correction factor is a function of the number of blades, the angle of relative wind, and the position on the blades

$$dT = \rho V1\,[4a\,(1 - a)\pi rd \quad (3.20)$$

where F is always between 0 and 1 and the angle obtained from the inverse cosine function is considered to be in radians.

The forces generated from blade element theory should be rectified using the tip loss factor as indicated below, since the tip loss alters the forces derived from momentum theory (the forces derived from blade element theory stay intact).

$$dT = F\rho V_1^2\ [4a\ (1-a)\ \pi dr \tag{3.21}$$

$$dQ = 4Fa'(\ 1-a\ )\rho V1\ \pi r^3 dr \tag{3.22}$$

We discovered the following relationships by equating these equations with those from blade element theory:

$$\frac{a'}{(1-a)} = \frac{\sigma' \times Cl}{4F\lambda r sin\varphi} \tag{3.23}$$

$$\frac{a}{(1-a)} = \frac{\sigma' \times Cl \times cos\varphi}{4Fsin2\varphi} \tag{3.24}$$

$$Cl = 4 \times F \times sin\varphi \frac{(cos\varphi - \lambda r sin\varphi)}{\sigma'(Sin\varphi + \lambda r cos\varphi)} \tag{3.25}$$

$$\frac{a'}{1+a'} = \frac{\sigma' \times Cl}{4Fcos\varphi} \tag{3.26}$$

$$a = \frac{1}{\left[1 + \frac{4 \times Fsin2\varphi}{(\sigma' \times Cl \times cos\varphi)}\right]} \tag{3.27}$$

$$a' = \frac{1}{\left[\left(\frac{4 \times Fcos\varphi}{(\sigma' \times Cl)}\right) - 1\right]} \tag{3.28}$$

$$Vrel = \frac{V(1-a)}{sin\varphi} = \frac{V}{\left(\frac{\sigma' \times Cl}{4F}\right) cot\varphi + sin\varphi} \quad (3.29)$$

Therefore, the power coefficient can be calculated as equation 3.30 or equation 3.31.

$$C_P = (\frac{8}{\lambda^2}) \int_{\lambda h}^{\lambda} F\lambda r^3 \times a'(1-a)[1-\left(\frac{Cd}{Cl}\right) cot\varphi] d\lambda r \quad (3.30)$$

$$CP = (\frac{8}{\lambda^2}) \int_{\lambda h}^{\lambda} Fsin^2\varphi (cos\varphi - \lambda_r sin\varphi)(sin\varphi + \lambda_r cos\varphi)[1-\left(\frac{Cd}{Cl}\right) \times cot\varphi] \lambda^2 d\lambda r \quad (3.31)$$

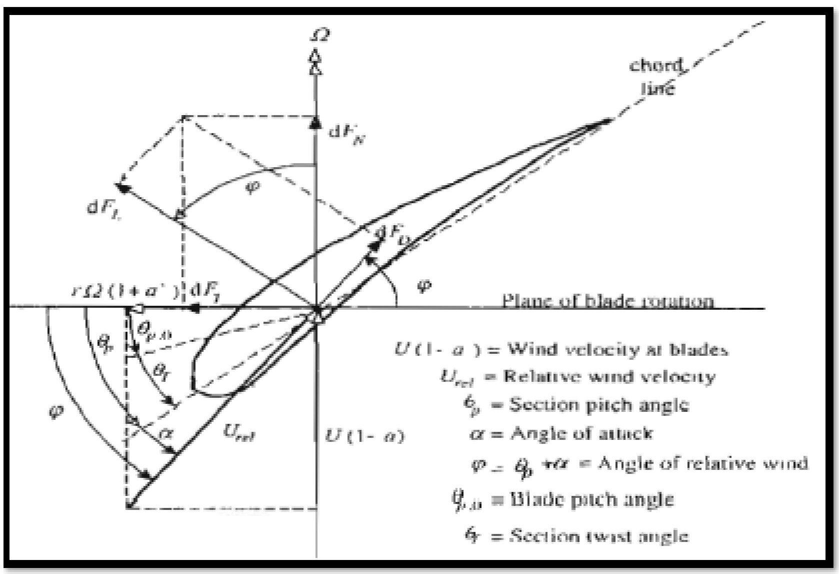

Figure 3.0.2:- Blade Element Theory, Geometry of the Airfoil (20)

The Horizontal axis wind turbine blade flow state.

The results of BEM theory closely match the behavior of real wind turbines at low axial induction factors. Since the far wake wind velocity would be negative at axial induction factors larger than 0.5, the general momentum theory is no longer relevant. The wind turbine flow pattern will become more complex than what the momentum theory might predict, even though the induction factor may actually be greater than 0.5. A rotor can function in a number of distinct states. The two operational states that are relevant to wind turbines are the design windmill state and the turbulent wake state. A wind turbine's normal operating state is known as the windmill state. The turbulent wake state occurs when operating in strong winds. The windmill state is defined by the flow conditions described by momentum theory for axial induction factors less than about 0.5. According to measured results, in the turbulent wake condition above a=0.5, thrust coefficients increase to about 2.0 at an axial induction factor of 1.0. Turbulence, recirculation behind the rotor, and a significant slipstream expansion are characteristics of this state. Although the turbine behavior is no longer described by momentum theory, wind turbine behavior is frequently predicted using empirical links between CT and the axial induction factor.

As shown below, the axial induction factor and thrust coefficient in turbulent wake states are related empirically using a model developed by Glauert that accounts for the tip loss factor.

$$\alpha = \left(\frac{1}{F}\right)\left[0.143 + \sqrt{0.0203 - 0.64279(0.889 - Ct)}\;\right] \quad (3.32)$$

It is valid for α > 0.4 or CT > 0.96.

It was demonstrated that the Glauert empirical connection applied to a rotor's overall thrust coefficient. It is typical to presume that it applies equally to identical local thrust coefficients for each part of the blade. The local thrust coefficient for each annular rotor section was calculated as follows;

$$CTr = \frac{dFN}{\frac{1}{2}\rho\, U^2 2\pi r dr} \quad (3.33)$$

From the blade element theory using the normal force relation the local thrust coefficient will be

$$C_{Tr} = \frac{\sigma'(1-a)^2\,(\mathrm{CLcos\varphi+CDsin\varphi})}{\mathrm{sin2\varphi}} \quad (3.34)$$

The design of turbine blades under heavy load and the power prediction of HAWTs running at high tip speed ratios can then be added to the solution process.

Blade Shape: Optimal Rotor Shape with Wake Rotation

When building a blade shape from a known airfoil type for an ideal rotor, it is important to determine the chord length distribution and twist distribution throughout the blade length for a given tip speed ratio at which the rotor's power coefficient reaches its maximum. It is possible to develop a general relationship between an ideal relative wind angle and local tip speed ratio that will work for all types of airfoils by applying the partial derivate of the integral relation for definition of CP, where Cd=0 and F=1.

$$\frac{\partial \sin 2\varphi \cos\varphi - \lambda r \sin\varphi\,(\sin\varphi + \lambda r \cos\varphi)}{\partial\varphi} = 0$$

After that we can find

$$\lambda_r = \frac{\sin\varphi(2\cos\varphi - 1)}{(1 - \cos\varphi\,(2\cos\varphi + 1)} \tag{3.35}$$

After more algebra than

$$\varphi = \left(\frac{2}{3}\right)\tan^{-1}(1/\lambda_r) \tag{3.36}$$

$$c = \frac{8\pi r}{BC_L}(1 - \cos\varphi) \tag{3.37}$$

To find the induction factor we can use

$$\acute{a} = \frac{1-3a}{4a-1} \tag{3.38}$$

$$a = \frac{1}{[1 + {}^{4\times\sin^2\varphi}\!/_{(\sigma\times C_l\acute{\times}\cos\varphi)}]} \tag{3.39}$$

The blade solidity is calculated by dividing the blade area by the swept area.

$$\sigma = \frac{1}{\pi R^2}\int_{r_h}^{R} c\,dr$$

(3.40)

$\sigma \cong \frac{B}{N\pi} (\sum_{I=1}^{N} \left(\frac{Ci}{R}\right)$

(3.41)

r = blade section radius, R = rotor radius, B = number of blades, C = airfoil chord length, and φ = tip speed ratio relative wind angle.

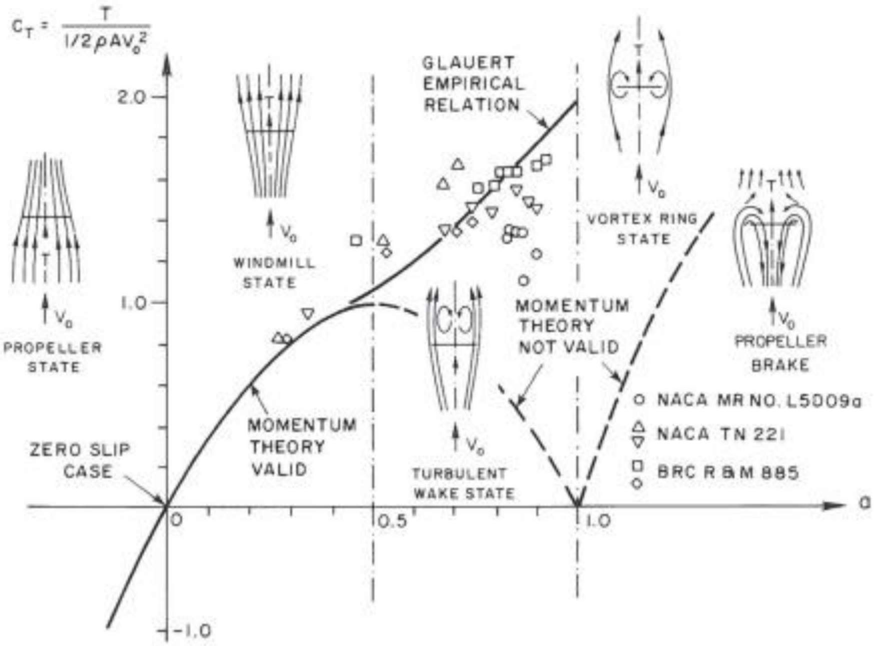

Figure 3.0.3:- Thrust coefficient (CT) as a function of average induction at the rotor plane (a). Figure from Eggleston and Stoddard

Wind Turbines 's Airfoil

HAWT blades have a simpler shape and flat plates for low tip speed ratios; an airfoil is employed to produce mechanical power for high tip speed ratios. The width and length of the blade are determined by the intended aerodynamic performance, the maximum planned rotor power, the anticipated airfoil characteristics, and strength estimates. Therefore, creating HAWT blades requires an understanding of airfoil properties.

The most significant factor affecting airfoil behavior is the viscosity of the fluid and airfoil combination, which is determined by the Reynolds number (Re) and is stated as follows. It is crucial to make sure that the appropriate Reynolds number data is used for the design since airfoils behave quite differently at different Reynolds numbers.

$$Re = \frac{V_{rel} \times C}{\vartheta} \tag{3.42}$$

The drag and lift characteristics of the airfoil also show a significant aspect ratio dependence for angles of attack larger than 30 degrees. At low angles of attack, however, two-dimensional (i.e., infinite aspect ratio) data can be used for blade design because aspect ratio has minimal impact on the fully attached region where HAWT functions in windmill form. However, when using two-dimensional data, a tip loss factor must be incorporated.

Wind turbine designers in the 1970s and early 1980s thought that optimizing blade twist and taper was far more important than making minor changes to airfoil performance characteristics (see [5]). Consequently, little attention was paid to the task of selecting aero foils. Aero foils that were already in use by the helicopter sector were chosen since it was believed that the helicopter was a similar application. Aviation aero foils such as the NACA 44xx and NACA 230xx were frequently employed because of their low pitching moment, low minimum drag coefficient, and high maximum lift coefficients.

The SG6043 airfoil was chosen for the current design because of its flat back geometry, which provides better performance and structural advantages, especially in the blade's inboard area. SG6042 and SG6040 airfoils have been used by other researchers in earlier investigations to alter blade thickness and improve structural and aerodynamic properties. While SG6043, with its sharp trailing edge, has been employed for aerodynamic efficiency, SG6042, a thicker airfoil, has generally been used in the mid-span region to boost bending stiffness and strength. Spar cap thickness is frequently graded transversely across the blade structure for increased resistance against external bending pressures.

Twist Distribution modification

A chosen blade shape must be twisted significantly, especially around the root, as is the case in the chord-length variation of the same blade, according to an analysis of the twist distribution.

As a result, twist distribution can be altered while accounting for manufacturing ease. The twist variation needs to be linearized across the blade length, just like the chord variation.

Determination basic rotor parameters

At this point, the basic characteristics will be determined. At the hub height, the wind speed is 6 m/s, the air density is set at 1.2 kg/m3, the overall electrical and mechanical efficiency is expected to be 90%, and the wind turbine power of 70 W calculated based on coefficient of performance Cp = 0.45 as calculated in chapter three. Therefore, using the following relation based on one-dimensional momentum theory, we can calculate the rotor radius

$$P = \frac{1}{2} \times C_p \times \rho \times \pi \times R^2 \times V^3 \quad (3.43)$$

where U is the mean wind speed at the hub height, which is 7 m/s, R is the blade's radius, which is 0.43 m, Cp is the expected coefficient of performance, which is 0.4 in the case of a three-bladed wind turbine, and η is the expected mechanical and electrical efficiency, which is 0.9.

$$p = \frac{1}{2} \times \times\ 0.45 \times 1.22 \times 3.14 \times (0.45)^2 \times (7)^3 = 74\ watt \quad (3.44)$$

The application region in which the wind turbine will be installed determines the tip speed ratio. Numerous publications indicate that stronger torque is needed for water pumping windmills, therefore a tip speed ratio of 1 to 3 is appropriate. For the production of electric power, a tip speed ratio of 4 to 10 is advised. Higher speed machines use less material in their blades but require more sophisticated airfoils. The system meant to be used for this thesis work is a direct drive arrangement with the generator, guaranteeing that the tip speed ratio is as high as possible because the power output of the generator is directly proportional to the rotor shaft's rotational speed. Additionally, the tip speed ratio has a major impact on the turbines' coefficient of performance; the figure below shows how they relate to one another using a common CP-λ.

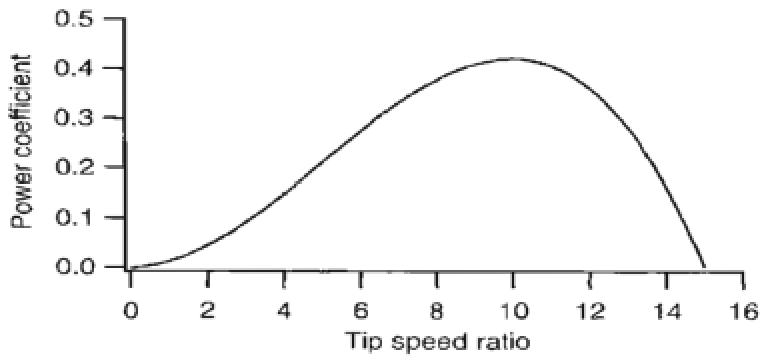

Figure3.4: Cp –**λ** sample curve for high tip speed ratio wind turbine(20)

As mentioned in this chapter's earlier sections, wind turbine design is an iterative process that aims to maximize rotor performance. The optimal tip speed ratio between 6 and 10 will be chosen at the end of the design procedure to provide us with the best performance for this thesis assignment.

Number of blades

The number of blades on a rotor also has a big impact on its performance. When choosing the number of blades for the rotor, the whole system's structural stability must also be considered. A single bladed wind HAWT will have a stronger thrust force at the upper position and a smaller one at the lower position due to the difference in wind speed between the two positions, which will increase the cycle stress. Furthermore, the absence of balance will cause instability in the hub, shaft, driving train, and tower; yet, single bladed wind turbines are less costly. Despite their high efficiency, stability, and solidity, multi-bladed wind turbines are less practical due to their high material and initial torque needs. When employing current production techniques, it is frequently desired to have as few blades as possible due to the fixed costs involved in generating the blades. These days, two or three blades are included on every commercial wind turbine. Furthermore, extra blades will be less rigid and can have higher strains at the roots for a given solidity. Most studies suggest the table below for determining the number of blades.

Table 3.1:Blade Number B, at different tip speed.

λ	**B**
1	8-24
3	6-12
3	3-6
4	3-4
>4	1-3

Airfoil selection

Based on a predetermined airfoil profile, this thesis aimed to create the ideal blade shape for achieving good performance. Among the many different types of standard airfoils are NACA, RISϕ, FFA, SG, S, DAE, Lissaman, and others. The primary selection criteria for the airfoil are a relatively high lift coefficient and a smaller drag coefficient. Modern large-scale wind turbines frequently employ multiple airfoils at different parts of the blade to improve performance and strength at the base.

Since the wind turbines to be built for this application are small-scale wind turbines, the use of a single airfoil with variable thickness and chord will improve the system's manufacturability. However, using different airfoils will cost a lot of money to manufacture and require advanced technology. But according to some studies, concentrating on the blade's design rather than the airfoil is a superior method to get good performance. NACA 230xx, NACA 44xx, NACA 63 2xx, SERI 804-808, DAE 21 and 11, and Lissaman 7769 are compared among the various airfoil profiles.

The final stage is to employ the previously indicated iterative procedures to get the optimal blade form, as the fundamental components of the design have already been selected. The design is based on the best blade shape prediction technique suggested by.

Initially, the blade must be separated into N portions along its span; the more sections, the more precise the output will be. Since the blade is just 0.43 meters long, splitting it into 12 pieces will be a good option. The radius at each segment's center serves as the basis for all values that must be computed for each section. Each section's local speed ratio can be computed as

$$\lambda_i = \lambda \times (\frac{r_i}{R})$$

(3.45)

Additionally, the optimum relative wind angle is determined by

$$\varphi = \left(\frac{2}{3}\right)\tan^{-1}\left(\frac{1}{\lambda r}\right)$$

(3.46)

The chord of each section can be find

$$c = \frac{8\pi r}{BC_l}(1 - \cos\varphi)$$

(3.47)

The twist angle of each section can be find

$$\theta_{Ti} = \theta_{pi} - \theta_{po}$$

(3.48)

Each section's pitch angle can be found.

$$\varphi_i = \theta_{pi} + a_{Design\ i}$$

(3.49)

The ratio of the minimum drag to lift coefficient needs to match the design angle of attack.. The angle of attack of the design should be equal to 80% of the maximum lift coefficient, according to the majority of literature. For various airfoils and tip speed ratios, the design procedure involves a lot of repetitive iteration.

Determination of performance of the rotor

In order to get the desired blade shape, the rotor's performance is assessed iteratively. The blade performance equation can be solved in two ways, as was indicated in the sections before this one: method one and method two. For this thesis work, the first option will be used; however, if the axial induction factor is greater than 0.5 throughout the iteration operations, approach two will be used.

Using equations 3.25, 3.26, and 3.27, this method solves the real CL and the angle of attack for the center of each section.

$$\sigma = \frac{B \times C_l}{2\pi r_l} \tag{3.50}$$

Based on the optimal relative wind angle, the lift coefficient, blade solidity, and tip loss factor are calculated. Next, ascertain the actual angle of attack using the airfoil profile curve for the Cl and α. Lastly, calculate the updated relative wind angle using the following relation.

$$\varphi_{i\,f+1} = \theta_i + a_{if} \tag{3.51}$$

where "i" is the section number and "j" is the number of iterations.

Use the following relation, determine the axial and angular induction factors till the difference between the succeeding iteration values,

$$a = \frac{1}{\left[1 + \frac{4 \times F sin 2\varphi}{(\sigma\prime \times Cl \times cos\varphi)}\right]} \tag{3.52}$$

$$a' = \frac{1}{\left[\left(\frac{4\times F\cos\varphi}{(\sigma'\times Cl)}\right)-1\right]}$$

(3.53)

After the iteration is finished, use the following relation to determine the blade's coefficient of performance.

$$CP = \left(\frac{8}{\lambda^{2}}\right)\int_{\lambda h}^{\lambda} F\sin^{2}\varphi\,(\cos\varphi - \lambda_r\sin\varphi)(\sin\varphi + \lambda_r\cos\varphi)[1 - \left(\frac{Cd}{Cl}\right)\times \cot\varphi]\lambda^{2} d\lambda r \quad (3.54)$$

3.3 Structural analysis

The simplified load model, aero elastic modelling, and mechanical load testing are the two primary methods for analyzing tiny wind turbines, according the International Electrotechnical Commission's document (IEC 6400-2, Design Requirements for tiny Wind Turbines).

*Table 3.2**:** Wind class*

parameters	**Class I**	**Class II**	**Class III**	**Class IV**
Reference wind speed	50	42.5	37.5	30
Annual Average wind speed	10	8.5	7.5	6
50 Years Return Gust Speed	70	59.5	52.5	42
1 Year Return Gust Speed	52.5	44.6	39.4	31.5

The simplified load model is the most appropriate and compatible with the system topology we are working on, and turbine configurations that can use it must satisfy all of the following criteria.

- ✓ Rotor with a horizontal axis,
- ✓ A propeller-type rotor with more than two or more blades,
- ✓ Cantilever blades, and
- ✓ A neither hinged nor steering rigid hub.

The turbine arrangement can be either upwind or downwind, run at variable or constant speed, have either a fixed pitch or an active or passive pitch mechanism, and furl around the vertical, horizontal, or intermediate axes or not.

Keep in mind that "F" is the fatigue loading analysis and "U" is the ultimate load study, which includes tip deflection, stability analysis, and surpassing the maximum material strength. If the indicated design condition calls for it, more load cases could be included. The design loads for various load scenarios and generated stresses are calculated in the ensuing sections.

Glass and carbon fiber composites (GFRP and CFRP) have a substantially higher compressive strength to weight ratio than the other materials, as is evident. Nevertheless, this seeming advantage is not as important as it initially appears for two reasons. First, the fibers of some of the plies that comprise the laminated blade shell must be orientated off axis, typically at a 45-degree angle, in order to sustain shear stresses. As a result, the axial strengths drop. Second, because these composites have relatively low Young's modulus, the design is controlled by resistance to buckling of the thin skins rather than simple compression yielding.

Table 3.3: Design load and stress requirements

Design situation	load cases	Wind inflow	Analysis
power production	A. normal operation		F
	B. Yawing	V_{hub}= V_{design}	U
	C. C Yaw Error	V_{hub}= V_{design}	U
	D. C Maximum thrust	V_{hub}= 2.5 V_{aver}	U
Power production plus	E. D Maximum rotational Speed		U
Occurrence of fault	F. E short at load connection	V_{hub}= V_{design}	U
Shutdown	G. F shutdown (braking)	V_{hub}= V_{design} V_{hub}= V_{e50}	U
Parked, idle or stand still	H. G parked wind loading		U
Parked and fault	I. H parked wind loading	V_{hub}= V_{Ref}	U
Transport, assembly and maintenance	J. I to be stated by manufacturer		U

Buckling will be less likely to occur in materials with high values, such as fake banana fiber composite, because the likelihood that buckling will occur is inversely proportional to the planar stability parameter., $E= (UCS)^2$.

$$\sigma_{M,B} = \frac{5.12}{3.0359 \times 10^{-6}} + \frac{21.4}{1.527 \times 10^{-4}} = 3.08\ Mpa$$

Blade design Parameters and materials properties

The following data are the blade design data which is used to determine the structural design of the blade

Table 3.4: - Blade design data

Parameter	Symbol	Value	Unit
Blade length	L	0.43	M
Number of Blade	N_b	3	-
Blade Root Chord	C_r	0.115	M
Blade Tip Chord	C_t	0.018	M
Root Thickness	Rt	0.016	M
Tip thickness	Tt	0.0018	M
Tip Speed Ratio	Λ	6	-
Wind velocity	V	7.5	M/S
Power coefficient	Cp	0.45	-
Airfoil	SG6043	SG6043	-
Materials	Enset	-	-
Material Density (Enset)	ρ_{Enset}	1250	Kg/m3
Air Density	P	1.22	Kg/m3
Ultimate Tensile	$\boldsymbol{\sigma}_{Ulti}$	60	Mpa
Youngs Modulus	E	6	Mpa
Allowable stress (IEC safety factor ≈ 1.5–2)	$\boldsymbol{\sigma}_{Allow}$	30	Mpa

Blade Geometry Approximation

Mean Chord

$$C_{Mean} = \frac{C_r + C_t}{2} \quad (3.55)$$

$$= \frac{0.115 + 0.018}{2} = 0.0665m$$

Mean Thickness

$$T_{mean} = \frac{t_r + t_t}{2} \quad (3.56)$$

$$T_{mean} = \frac{0.016 + 0.018}{2} = 0.0089m$$

- **Power out put**

$$P = \frac{1}{2} \times C_p \times \rho \times \pi \times R^2 \times V^3 \quad (3.57)$$

$$= \frac{1}{2} \times\times 0.45 \times 1.22 \times 3.14 \times (0.45)^2 \times (7.5)^3 = 74\ watt$$

- **Angular velocity of the blade**

$$\omega = \frac{\lambda V}{R} \quad (3.58)$$

$$= \frac{6\ x7.5}{0.45} = 100\ rad/s$$

- **Blade Volume**

$$V = b \times h \times l \quad (3.57)$$

The means of the blade base and height are average thickness and chord of the blade respectively

$$V_{blade} = 0.0665 \times 0.0089 \times 0.45 = 2.66 \times 10^{-4}\ m3$$

- **Mass of the blade**

The mass of the blade (M_b) is found based the volume of the blade and the density of the materials

$$Mb = \rho \times Vb \quad (3.58)$$

$$= 1250 \times = 2.66 \times 10^{-4}\ m3 = 0.33Kg$$

Rcog = 700rpm = 73.3rad/s, Rcog, max = 1000rpm =104.2rad/s , V$d$esign = 10.5 m/s, Design = 10.7rad/s

Load cases of the blade

I. Load cases A: normal Oeration

Equation following provides the centrifugal load and includes two parameters that have been established. Weighing or using CAD or finite element software for pre-manufacturing study makes it simple to determine the blade mass, or mB. As an alternative, it is simple to alter the analysis for the moment of inertia in the above to obtain mB. With a density of 1250 kg/m3, the aforementioned blades have a current of mB = 0.33 kg. Similar methods can be used to calculate the blade's center of mass, or Rcog, although it should be noted that the hub end of the blade is unlikely to match zero radius. Rcog is 0.225 m in this instance. So,

$$\Delta \boldsymbol{F}_{ZB} = \boldsymbol{2m}_B \ \boldsymbol{R}_{cog} \ \omega^2_{n\,design} \tag{3.59}$$

$$= 2 \times 0.33 \ \times 0.225 \times \ 73.33^2 = \ 798.5 \ N$$

$$\Delta \boldsymbol{M}_{XB} = \frac{Q_{Design}}{B} + \ \boldsymbol{2m}_B \ g \ \boldsymbol{R}_{cog} \tag{3.60}$$

$$= \frac{10.7}{3} + 2 \times 0.33 \times 9.81 \times 0.225 = 5.12 \ NM$$

$$\Delta M_{yB} \ = \lambda_{Design} \ \frac{Q_{Design}}{B} \tag{3.61}$$

$$= 6 \times \frac{10.7}{3} = 21.4NM$$

$$\Delta \text{Fx shaft} = 3 \times \frac{\lambda\text{design} \times \text{Qdesign}}{2R} \tag{3.62}$$

$$= \frac{3 \times 6 \times 10.7}{2 \times 0.45} = 214N$$

Using measured rotor mass $M_r = 2.9$kg , and $e_r = 0.005 \times 0.45 = 0.00225$ m, and

$$\Delta \boldsymbol{M}_{XShaft} = Qdesign + 2M_r g e_r \quad (3.63)$$

$$= 10.7 \times 2 \times 2.99 \times 9.81 \times 0.00225 = 10.8NM$$

The additional shaft moments are calculated using the intended length between the rotor and the first bearing, assuming that eccentricity has minimal influence in this situation. $L_r = 0.026m$.

$$\Delta \boldsymbol{M}_{Shaft} = 2M_r g l_{rb} + \frac{R}{6}\ \Delta\text{Fx shaft} \quad (3.64)$$

$$= 2 \times 2.99 \times 9.81 \times\ 0.026 + \frac{0.45}{6} \times 214 = 17.57nm$$

II. ***Load case B:- Yawing***

The extra factors determine the blade root bending moment. *Lrt* = 0.099 m, the distance from the rotor to the yaw axis, and *JB*,= the blade moment of inertia, $JB = mBRcog^2 = 0.33 \times 0.225^2 = 0.0167\ Kgm^2$

$$M_{YB} = M_B\ \omega_{yaw}^2 LrtRcog + 2\omega yawIB\omega n + \frac{R}{9}\Delta Fx\ shaft \quad (3.65)$$

While maximum yawing is fin by using

$$\omega_{yaw\,max} = 3 - 0.01\ (\pi R^2 - 2)$$

$$\omega_{yaw\,max} = 3 - 0.01\ (\pi R^2 - 2) = \ 3.01\ ras/s \quad (3.66)$$

$$M_{YB} = 0.33 \times 3.01^2\ \times 0.099 \times 0.225 + 2 \times 3.01 \times 0.0167 \times 73.3 + \frac{0.45}{9} \times 214$$

$$18.13\ nm$$

Similarly given the shaft moment as

$$\boldsymbol{M}_{Shaft} = N\omega_{yaw}\Omega JB + M_r gLrt + \frac{R}{9}\Delta Fx\ shaft$$

$$= 3 \times 3.01 \times 0.0167 \times 73.3 + 2.99 \times 9.81 \times 0.099 + \frac{0.45}{9} \times 214 \quad (3.67)$$

$$= 24.6\ nm$$

III. *Load case C: YAW ERROR*

A value for $A_{\text{proj, }B.}$ = 0.06850m2 is required for airfoil SG6043 and Cl max = 1 This can be done using a modification of the analysis

$$M_{yB} = \frac{1}{8}\rho A_{proj,B} C_{l\ max}\ R^3 \Omega_{Design}^2 \left[1 + \frac{4}{3\lambda_{design}} + \left(\frac{1}{\lambda_{design}}\right)^2\right] \quad (3.68)$$

$$= \frac{1}{8} 1.22 \times 0.06850 \times 2 \times 0.45^3 \times 73.3^2 \left[1 + \frac{4}{3 \times 6} + \left(\frac{1}{6}\right)^2\right] = 12.78Nm$$

IV. *Load case D: Maximum thrust*

Using the below equation, the calculation is straightforward

$$F_{x-shaft} = 3.125 C_T \rho U_{Ave}^2\ \pi R^2 \quad (3.70)$$

$$= 3.125 \times 0.45 \times 1.22 \times 7.5^2 \times 3.14 \times (0.45)^2 = 61.36\text{N}$$

V. *LOAD CASE E: maximum rotational Speed*

Using the following formula, the centrifugal loading at the blade root can also be easily calculated. while $\omega_{n\ max}^2 = 1000rpm = 104.72\ rad/s$

$$F_{ZB} = M_B\ R_{Cog}\ \omega_{n\,max}^2 \quad (3.71)$$

$$= 0.33 \times 0.225 \times (104.72)^2 = 814.24N$$

The shaft bending moment is found by using Equation below

$$M_{shaft} = M_r g l_{rb} + M_r e_r\ \omega_{n\,max}^2 \quad (3.72)$$

$$= 2.99 \times 9.81 \times 0.099 + 2.99 \times 104.72^2 \times 0.00225$$

$$= \mathbf{76.67} Nm$$

VI. *Load case F: - short at load connection*

Now think about the burden brought on by a generator short circuit. G = 2 is the short circuit torque factor since the turbine has a permanent generator. So,

$$M_{X-shaft} = GQ_{design} \quad (3.73)$$

$$= 2 \times 10.7 = 21.4\ Nm$$

$$M_{x,B} = \frac{M_{X-shaft}}{N} \quad (3.74)$$

$$= \frac{21.4}{3} = 7.1NM$$

VII. *LOAD CASE H: Parking Wind*

At a wind speed of Ue50, this wind loading is imparted to the parked turbine. The turbine is presumed to have furled, and the blades are essentially motionless. The blades will not be normal to the wind direction due to the furling, hence the bending moment will be overestimated if we use the equation below with a predicted blade area of 0.06850m2 and Cd = 1.5 cl = 2.

$$M_{y,B} = \frac{1}{4} \text{Cd } \rho \text{V}_{e50}^{2} \text{Aproject BR} \quad (3.74)$$

$$\frac{1}{4} \times 1.5 \times 52.5^{2} \times 1.22 \times 0.06850 \times 0.45 = 621.9 \text{ Nm}$$

$$F_{x-shaft} = \frac{1}{2} N C_{d} \, \rho U_{e50}^{2} \text{Aproject B} \quad (3.75)$$

$$= \frac{1}{2} \times 1.5 \times 3 \times 1.22 \times 52.5^{2} \times 0.06850 = 518.26 NM$$

E. Blade Stress

A. LOAD CASE A: Normal operation

IEC 61400-2 states that the fatigue study solely takes into account load case A. The following are the stresses brought on by load case A.

Axial stress

$$A_{B} = 4.09 \times 10^{-4} \, m^{2}$$

$$W_{x,B} = 4.09 \times 10^{-4} \, m^{2}$$

$$\sigma_{z,B} = \frac{\Delta F_{Z,B}}{A_{B}} \quad (3.76)$$

$= \frac{798.5 \, N}{4.09 \times 10^{-4} \, m^{2}} = 1.952\text{Mpa}$

Bending Stress

$$\sigma_{M,B} = \frac{M_{x,B}}{W_{x,B}} + \frac{M_{Y,B}}{Wy_{,B}} \quad (3.77)$$

The values of the $W_{x,B} = 3.0359 \times 10^{-6}, Wy_{,B} = 1.527 \times 10^{-4}$ so that

$$= \sigma_{M,B} = \frac{5.12}{3.0359 \times 10^{-6}} + \frac{21.4}{1.527 \times 10^{-4}} = 1.85\ Mpa$$

$$\sigma_{eq} = \sigma_{z,B} + \sigma_{M,B} \tag{3.78}$$

$$= 1.952 + 1.85 = 3.802 Mpa$$

(60) states that the formula can be used to determine the maximum equivalent stress at which the material won't fail from fatigue.,

$$\sigma_{eq,Max} = \frac{\sigma_t}{Fs} \tag{3.79}$$

$$= \frac{60Mpa}{2} = 30\ Mpa$$

Because the fatigue design stress is greater than the generated fatigue stress, the blade won't fail due to fatigue.

Load case B: Yawing

Equivalent Stress for Case B: Yawing

$$\sigma_{M,B} = \frac{M_{Y,B}}{Wy_{,B}} \tag{3.80}$$

$$\sigma_{M,B} = \frac{18.13}{= 1.527 \times 10^{-4}} = 0.118 Mpa$$

Load case C: Yawing Error

$$\sigma_{M,B} = \frac{M_{Y,B}}{Wy_{,B}} \tag{3.81}$$

$$= \frac{12.27}{1.527 \times 10^{-4}} = 8.03 MPA$$

Load Case E: Maximum Rotational Speed

$$\sigma_{eq} = \frac{F_{ZB}}{A_B} \tag{3.82}$$

$$= \frac{814.2}{4.09 \times 10^{-4}} = 1.99Mpa$$

Load case F: Short at Load Connection

$$\sigma_{M,B} = \frac{M_{x,B}}{W_{x,B}} \tag{3.83}$$

$$= \frac{7.1}{3.0359 \times 10^{-6}} = 2.338Mpa$$

Load case G: Shutdown (Braking)

$$\sigma_{M,B} = \frac{M_y}{I} \tag{3.84}$$

$$\frac{3.35}{3.0359 \times 10^{-6}} = 1.1Mpa$$

Load case H: Parked Wind Loading

$$\sigma_{M,B} = \frac{M_{Y,B}}{Wy_{,B}} \tag{3.85}$$

$$= \frac{621.9}{1.527 \times 10^{-4}} = 4.07\ Mpa$$

3.4 Blade structural optimization using Solidworks software

Numerical Method Used in SolidWorks Simulation

To assess and optimize structural elements under various loading scenarios, SolidWorks Simulation uses an iterative optimization approach based on stress in conjunction with the Finite

Element Method (FEM). Stresses, displacements, and safety factors are obtained by numerically solving equilibrium equations after the blade geometry is discretized into finite elements. The controlling FEM formula is written as.

$$F = [K]\{u\} \tag{3.86}$$

Whare

- K= Global stiffness matrix
- u = Nodal Displacement Vector
- Applied Force Vector

Th Stress in each Elements is calculated by using

$$\{\sigma\} = [D]\{\mathcal{E}\} \tag{3.87}$$

Where [D] represents the Constitutive Matrix of Enset Fiber materials

Optimization Algorithm in SolidWorks

SolidWorks uses a **gradient-based design optimization approach**, where the design variables are iteratively modified to satisfy safety constraints while minimizing stress or mass.The optimization objective is defined as minimizing the maximum stress:

$$Min\ F(x) = \sigma_{Max} \tag{3.88}$$

Subject to constraint of

$$\sigma_{Max} \leq \sigma_{allowable} \tag{3.89}$$

Factor of safety is Computed as

$$FoS \leq \frac{\sigma_{allowable}}{\sigma_{Max}} \tag{3.90}$$

SolidWorks automatically evaluates the FoS for each load case and identifies critical regions.

CHAPTER FOUR

4. RESULT AND DISCUSSION

Chapter Four presents the overall results and discussion of the blade design and analysis. Section 4.1 describes the aerodynamic results, including the selection of the SG6043 airfoil, optimization of the tip speed ratio (6), chord and twist distribution, and the achieved power coefficient (Cp = 0.45). Section 4.2 explains the structural strength analysis under different load cases such as yawing, centrifugal, and parked conditions, showing that all stresses are within allowable limits with a minimum factor of safety of 3.7. Section 4.3 presents the SolidWorks simulation and optimization results, highlighting the fine mesh model, maximum von Mises stress at the blade root, and maximum displacement at the blade tip. The results confirm that the blade is both aerodynamically efficient and structurally safe. Overall, the chapter validates the suitability of the design for small-scale rural electrification applications.

4.1 Aerodynamic of the blade Result

SG6043 is chosen for this design after a preliminary analysis using Microsoft Excel 2007 is conducted to identify the best alternative airfoil. The iteration process was carried out for various tip speed ratios, between 5 to 7. where a comparison of the final coefficient of performance shows that 6 tip speed ratios are sufficient. Additionally, this system's design configuration is direct driven, resulting in a good 6 tip speed ratio. This is because the generator's power output is directly impacted by the rotor's rotation speed. The outcomes at this tip speed ratio are shown in the table below.

The chord distribution shown in Figure 3.4 illustrates a nonlinear decreasing trend from the blade root toward the tip, which is consistent with optimal aerodynamic blade design principles. The chord length is highest near the root (approximately 0.035 m at small radius values) and gradually reduces to about 0.004–0.005 m near the tip (around 0.4 m radius). This reduction in chord along the span is essential to balance aerodynamic loading and maintain an approximately uniform angle of attack under varying relative wind speeds. The larger chord at the root compensates for lower tangential velocity in that region, enhancing lift generation and structural strength where bending moments are highest. Conversely, the smaller chord at the tip reduces drag, minimizes material usage, and decreases centrifugal and bending stresses. The smooth tapering trend indicates proper aerodynamic optimization, likely derived from blade element momentum (BEM) theory, ensuring improved power coefficient and reduced structural loading. Such chord variation enhances both aerodynamic efficiency and mechanical stability, supporting the structural results where maximum stress was observed at the root and minimum stress at the tip. Overall, the obtained chord distribution confirms that the blade geometry follows theoretically optimized small-scale wind turbine design criteria suitable for rural electrification applications.

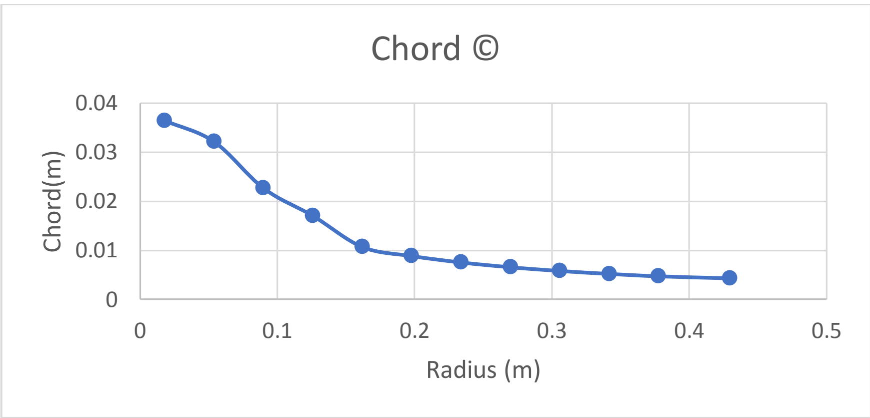

Figure 4.0.1: Chord vs Radius

The chord and twist distribution presented in Table 3.2 demonstrates a typical aerodynamic optimization trend for a horizontal-axis small-scale wind turbine blade based on blade element momentum (BEM) theory. The chord length decreases progressively from 0.115 m at the root (R/r = 0.045) to 0.018 m at the tip (R/r = 1), confirming a strong tapering profile designed to balance lift generation and structural loading. Similarly, the section twist reduces from 22.5° at the root to 0° at the tip, while the section pitch gradually transitions from positive values near the root to slightly negative values toward the outer span. This gradual reduction in twist is essential to maintain an optimal angle of attack along the blade span as the relative wind speed increases with radius. The local speed ratio increases consistently from 0.495 at the root to 11.385 at the tip, reflecting the expected rise in tangential velocity. These results align well with findings reported in recent studies on optimized small wind turbine blades, where chord and twist decrease nonlinearly from root to tip to achieve maximum power coefficient while minimizing aerodynamic losses (51)). Similar chord taper ratios and twist decay patterns were also observed in (52), who reported that higher root chord and twist improve torque generation, whereas reduced tip geometry lowers drag and bending stress. Therefore, the obtained distribution confirms that the blade geometry is aerodynamically optimized and structurally efficient, supporting both performance enhancement and stress reduction for rural electrification applications.

Table 4.1: - Chord and twist distribution

No.	radius(m)	local speed ratio	Phi	section pitch	section twist	R/r	Chord(m)
1	0.018	0.495	42.4431	39.4431	22.5	0.045	0.115
2	0.054	1.485	22.6376	19.6376	19.63	0.135	0.090
3	0.09	2.475	14.6671	11.6671	17.66	0.225	0.070
4	0.126	3.465	10.7321	7.7321	15.73	0.315	0.065
5	0.162	4.455	8.4342	5.4342	10.43	0.405	0.055
6	0.198	5.445	6.93778	3.93778	9.55	0.495	0.047
7	0.234	6.435	5.88875	0.08875	7.56	0.585	0.035
8	0.27	7.425	5.11363	-0.6864	5.25	0.675	0.030
9	0.306	8.415	4.51799	-1.282	4.55	0.765	0.028
10	0.342	9.405	4.04617	-1.7538	2.25	0.855	0.025
11	0.378	10.395	3.6633	-2.1367	1.5	0.945	0.020
Tip	0.45	11.385	3.34646	-2.4535	0	1	0.018

The number of sections is N. The design is repeated by modifying the parameters at the start of the design, such as the chord distribution or even the tip speed ratio, among other things, if the calculated performance is lower than anticipated. Using SB6043 airfoils, the tip speed ratio was examined from 5 to 7 for this design thesis, and the 6-tip speed ratio was selected beforehand. The outcome is displayed in the table below.

The optimization process carried out using Microsoft Excel 2013 resulted in a total power coefficient (Cp) of **0.45**, as shown in Table 4. The blade was divided into 12 sections using the SG6043 airfoil, and the sectional Cp values indicate a non-uniform contribution along the span. The highest contribution occurs at Section 4 (Cp = 0.269), followed by Sections 3 (0.193) and 2 (0.112), showing that the mid-span region plays a dominant role in overall energy extraction. In contrast, the root (Section 1, Cp = 0.026) and some outer sections exhibit lower contributions, which is consistent with aerodynamic theory where blade root regions experience lower relative wind speeds and higher structural constraints. The optimized total Cp of 0.45 is comparable to results reported in the literature for small horizontal-axis wind turbines using SG6043 airfoils, where Cp values typically range between 0.40 and 0.48 under optimal tip-speed ratios. For example, several blade element momenta (BEM) based studies report maximum Cp values around 0.42–0.47 for optimized small-scale rotors, indicating that the present Excel-based optimization approach provides competitive aerodynamic performance. Although the achieved Cp remains below the Betz limit (0.593), it demonstrates good agreement with practical turbine performance reported in previous experimental and numerical studies, confirming the reliability of the spreadsheet-based optimization method for preliminary wind turbine blade design.

Table 4.2: Total power coefficient Cp

SECTION	SECTION CP	Total Cp	Airfoil
1	0.026464427	0.45	SG6043
2	0.111863798		SG6043
3	0.193019402		SG6043
4	0.269389189		SG6043
5	0.0341867589		SG6043
6	0.0410821951		SG6043
7	0.0476408985		SG6043
8	0.0538633102		SG6043
9	0.059672681		SG6043
10	0.0642391419		SG6043
11	0.05904273		SG6043
12	0.08042701		SG6043

4.1 Structural analysis Result

Table 3.7 presents the strength analysis results for the blade under different critical loading conditions, including yawing (Load Case B), yaw error (Load Case C), maximum rotational speed (Load Case E), short at load connection (Load Case F), shutdown parking (Load Case G), and parked wind loading (Load Case H). The analysis shows that all computed stresses remain within allowable material limits, with factors of safety (FoS) ranging from 3.7 to 15, indicating that the blade structure satisfies strength requirements under both operational and extreme conditions.

Under yawing conditions (Load Case B), a flapwise bending moment of 24 Nm produces a bending stress of 3.9 MPa, resulting in a FoS of 7. Similarly, parked wind loading (Load Case H) generates a bending stress of 4.07 MPa with a FoS of 7, showing that flapwise bending during yaw-related and parked conditions governs the blade design. The yaw error case (Load Case C) yields the lowest FoS of 3.7, despite a relatively small bending stress of 0.4 MPa, indicating that misalignment conditions reduce structural safety margins more significantly than steady operational loads. This observation is consistent with recent findings reported in Composite Structures, where yaw misalignment was shown to amplify bending stresses and reduce safety margins in composite wind turbine blades.

For maximum rotational speed (Load Case E), the centrifugal force of 814.24 N induces a tensile stress of 1.99 MPa with a FoS of 15. This demonstrates that centrifugal loading is less critical compared to bending-dominated cases. Similar conclusions were reported in studies published in Renewable Energy and Energy Reports, where centrifugal effects produced tensile stresses but maintained relatively high safety factors compared to aerodynamic bending loads.

Edgewise bending conditions, such as short at load connection (Load Case F) and shutdown parking (Load Case G), produce stresses of 2.338 MPa and 1.1 MPa with FoS values of 12 and 15, respectively. These results indicate adequate structural resistance under transient and parked scenarios. Comparable stress distributions under edgewise loading have been documented in Journal of Renewable and Sustainable Energy, confirming that edgewise loads are generally less critical than flapwise bending in small to medium-scale wind turbine blades.

Overall, the present analysis demonstrates that yaw-related loading conditions are the governing design cases, while centrifugal and edgewise loads remain within safe structural limits. The minimum FoS of 3.7 exceeds the commonly recommended design threshold (2.5–3.0) for composite blade structures, suggesting that the blade design is structurally reliable and consistent with trends reported in recent literature.

Table 4.3: Result of the Strength Analysis for the Blades

Load case	Load type	Value	Stress type	Value	Factor of safety
Load case B: **Yawing**	Flapwise Bending Moment	24Nm	Bending Stress	3.9Mpa	7
Load case C: yaw error	Flapwise Bending Moment	12.78Nm	Bending Stress	0.4Mpa	3.7
Load case E: maximum rotational speed	Centrifugal Force	814.24N	Tensile Stress	1.99 Mpa	15
Load Case F: short at load connection	Edgewise Bending Moment	7.1Nm	Bending Stress	2.338 Mpa	12
Load Case G: shutdown parking	Edgewise Bending Moment	3.35Nm	Bending Stress	1.1Mpa	15
Load Case H: parked wind loading	Flapwise Bending Moment	621Nm	Bending Stress	4.07	7

4.3 Solidworks Optimization Result

In this study the Blade ware modeled and optimized in solid works software by using meshing Fine. The Normal operation case has been selected for optimization and it shows the blade's maximum Von mises Stress are exactly blade root while the maximum displacement at blade's Tip which shows good with standing design as shown in the figure below.

Figure 5 presents the structural simulation results of the small-scale wind turbine blade modeled and analyzed using SolidWorks Simulation. Figure 5A shows the fine mesh applied to the blade geometry, ensuring accurate stress and displacement prediction along the span, particularly near the root region where stress concentration is expected. A refined mesh was adopted at the root–hub interface to capture the stress gradient accurately, as this region typically experiences maximum bending loads due to aerodynamic and centrifugal forces.

The von Mises stress distribution (Figure 5B) indicates that the maximum stress occurs at the blade root, while the stress gradually decreases toward the tip. The peak stress value is approximately 7.13×10^6 N/m^2 (7.13 MPa), which is significantly lower than the typical tensile strength range of natural fiber–reinforced polymer composites (20–80 MPa depending on fiber treatment and resin type). This confirms that the blade structure remains within safe limits under the applied loading condition. The stress concentration at the root is consistent with classical cantilever beam behavior of horizontal-axis wind turbine blades, as also reported in recent studies on small-scale composite blades (52) where maximum stresses were observed at the blade root due to bending moments induced by aerodynamic loading.

The displacement result (Figure 5C) shows that the maximum tip deflection is approximately 0.478 mm, occurring at the free end of the blade. The displacement gradually reduces toward the root, which remains nearly fixed due to boundary constraints. The magnitude of tip deflection is relatively small compared to the blade length, indicating sufficient stiffness of the enset fiber–resin composite structure. Recent experimental and numerical investigations on natural fiber composite blades (53) reported comparable deformation patterns, where tip displacement remained below 1 mm for laboratory-scale blades under similar loading conditions. This suggests that the present blade design achieves adequate rigidity while maintaining lightweight characteristics.

Compared to conventional glass fiber blades, the obtained stress and deformation values demonstrate that Enset fiber composite can provide acceptable structural performance for small-scale wind applications. (51) highlighted that while synthetic composites offer higher strength, natural fiber composites can achieve sufficient mechanical performance for low-capacity turbines with the added advantages of biodegradability, reduced cost, and lower environmental impact. The current results align with this conclusion, confirming that the optimized geometry combined with appropriate resin–hardener ratio and gelcoat finishing enhances structural stability.

Overall, the simulation results validate that maximum stress occurs at the blade root, maximum displacement occurs at the blade tip, and both values remain within acceptable safety margins. The structural behavior follows expected theoretical trends for cantilevered wind turbine blades. Therefore, the designed Enset fiber–reinforced blade is structurally safe and suitable for rural electrification applications, offering a sustainable alternative to conventional synthetic composite blades.

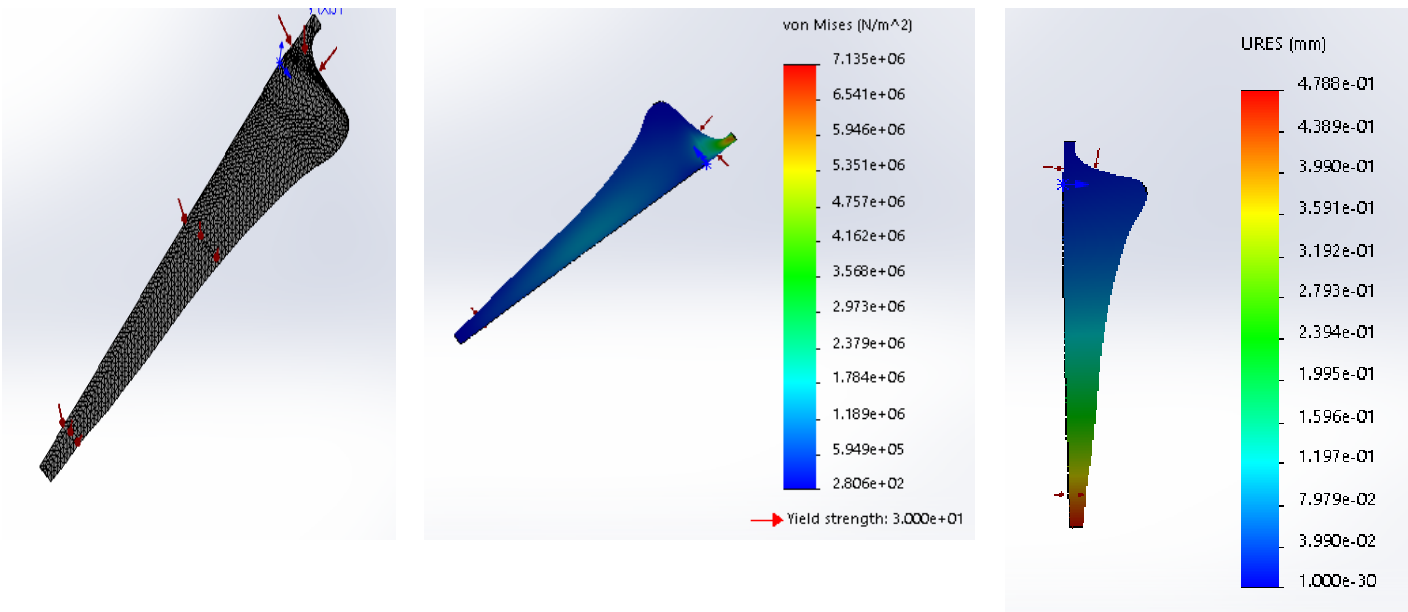

A B C

Figure 4.0.2:- A= fine meshed Blade, C= The stress result C= Displacement Result

CHAPTER FIVE

5.MANUFACTURING

This section explains how a small-scale horizontal-axis wind turbine blade made of Enset (false banana) fiber reinforced polymer composite is manufactured. Aerodynamic blade design, composite mold creation, additive manufacturing for pattern creation, and final blade lay-up and polishing are all integrated into the process. The approach adheres to well established wind turbine design concepts and composite fabrication techniques documented in credible literature (54).

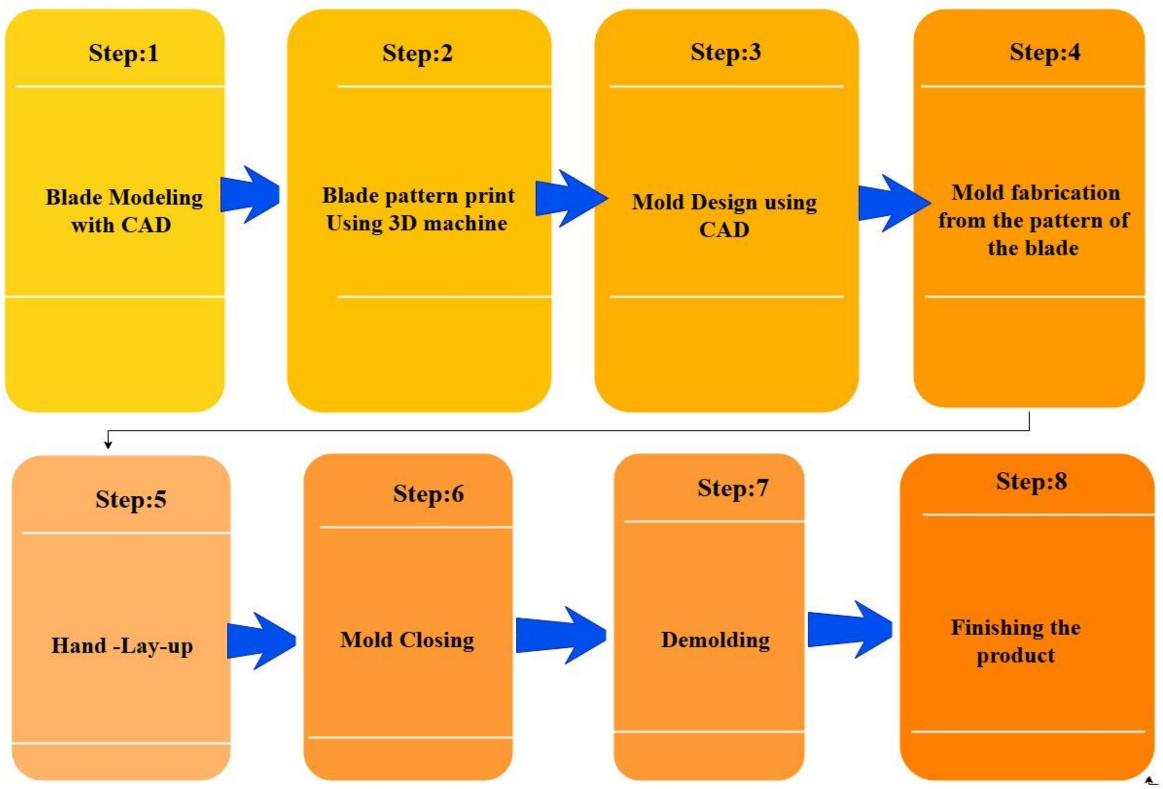

Figure 5.1: - Manufacturing Process Diagram

5.1 Manufacturing process

5.1.1 AERODYNAMIC BLADE DESIGN AND CAD MODELING

The aerodynamic design of the blade was based on the SG6043 airfoil shape, which is suitable for small-scale wind turbine applications and has a strong lift-to-drag ratio at low Reynolds numbers.(54). The necessary blade length and aerodynamic twist were incorporated into a solid three-dimensional model of the blade. The master geometry for structural analysis and mold development was this CAD model. The three-dimensional blade model created in SolidWorks using SG6043 airfoil coordinates as shown the figure below.

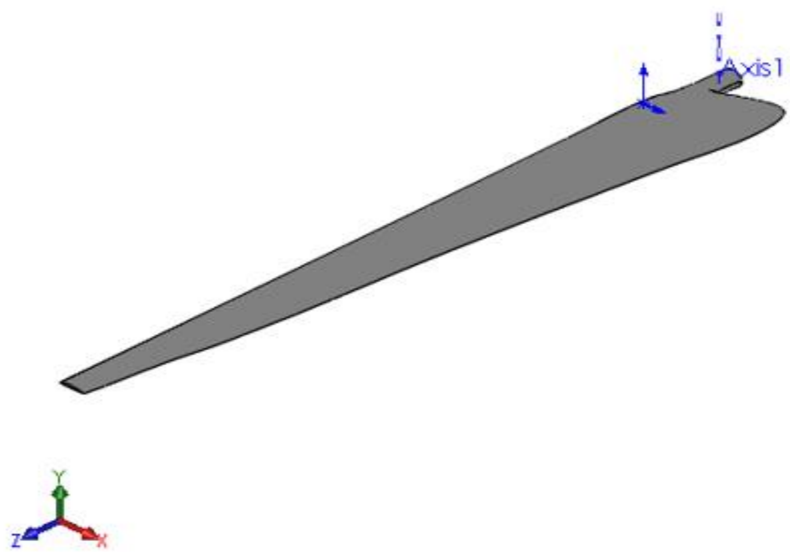

Figure 5.2: - Blade Model

5.1.2 PREPARING BLADE PATTERNS WITH 3D PRINTING

The completed CAD model of the blade was exported in STL format and then integrated into the Cura slicing program. The dimensional stability, low shrinkage, and applicability of polylactic acid (PLA) filament for quick prototyping in composite mold manufacturing led to its selection (54). As suggested by additive manufacturing studies, the blade pattern was manufactured using a 3D printer a kind of fused deposition modelling (FDM) 3D printer with an infill density of 20%, which offers sufficient stiffness while requiring less material and printing time(54). The blade model setup in Ultimaker Cura 5.11.0 version software and the finished 3D-printed blade pattern are shown in the **figure** below.

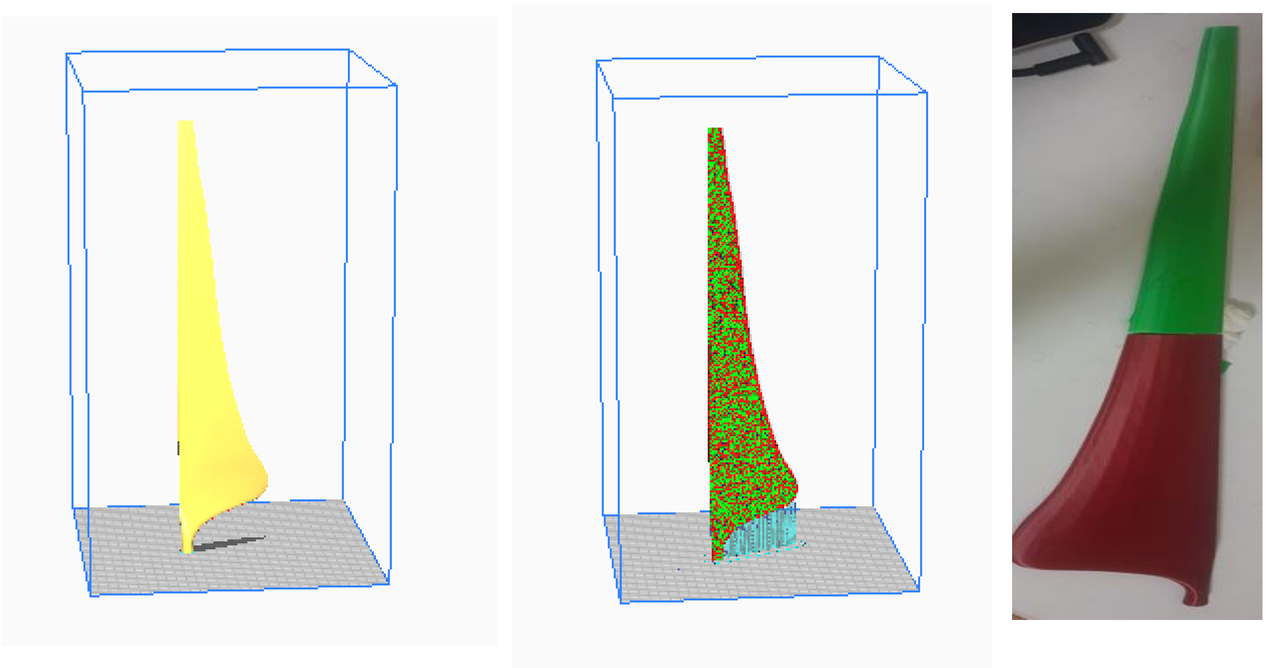

A B C

Figure 5.3:- (A) Blade inserted Ulimaker Cura, B= Sliced blade in Cura, C= printed Blade using PLA material

5.1.3 Mold Design

SolidWorks' Mold Tools feature was used to design a split mold based on the blade geometry. To make upper and lower mold halves, the blade was split along the separation plane. To make demolding easier, draft angles and parting lines were established in accordance with conventional composite mold design recommendations(55). The mold cavities were designed with sufficient thickness and alignment features to ensure dimensional accuracy and repeated usability. **Figure** below shows the upper and lower cavity mold design generated in SolidWorks.

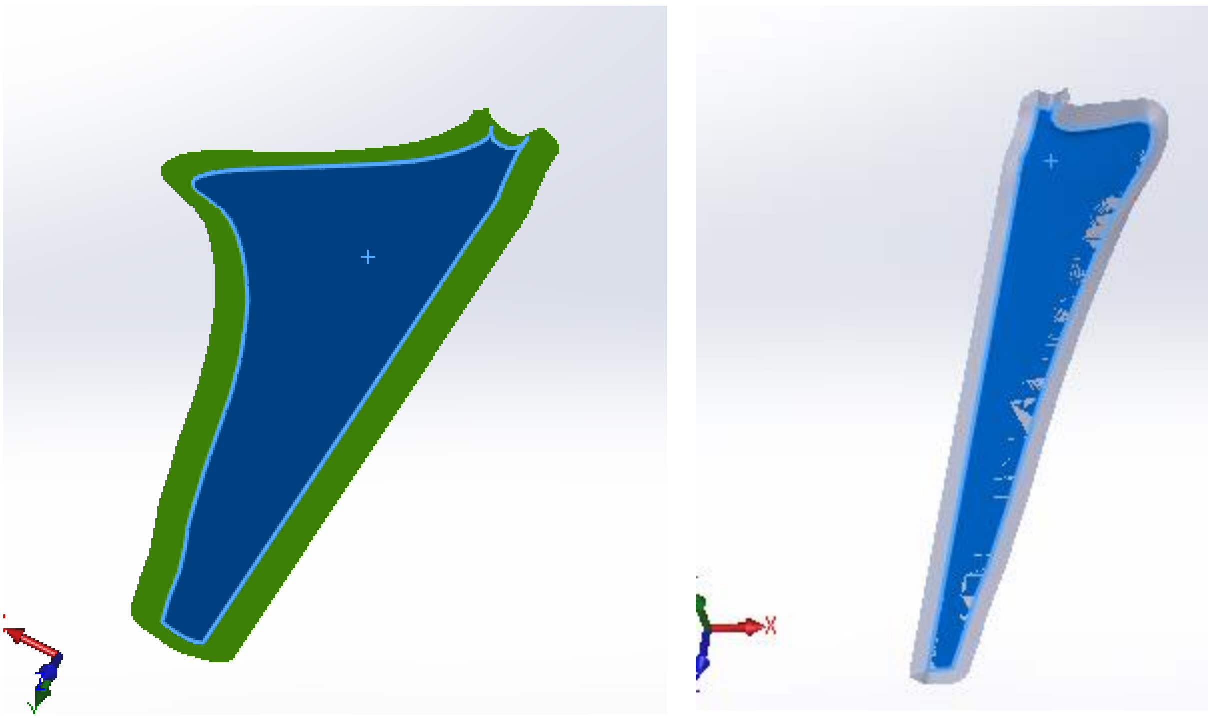

A B

Figure 5.3: - A= upper part mold, B= bottom Part Mold

5.1.4 Fabrication of Composite Mold Using Fiber and Resin

The composite mold was fabricated using the 3D-printed blade pattern as a master model. The pattern surface was sanded, polished, and coated with multiple layers of mold release wax to prevent adhesion(55). To create a smooth mold surface, a layer of gelcoat was applied. Layers of fiber reinforcement were added and saturated with resin combined with the proper hardener once the gelcoat had become tacky. In accordance with hand lay-up mold production methods documented in the literature, the laminate was cured at room temperature(56). The Manufuctured composite molds is shown in the **figure** below.

Figure 5.4: - Manufactured Mold

5.1.5 Preparation of Enset Fiber Reinforcement

Because of its availability, biodegradability, and advantageous mechanical qualities, Enset (false banana) fiber was chosen as a natural reinforcement material. As suggested for natural fiber composites, proper fiber orientation along the blade span was maintained to enhance tensile and bending performance (56). The prepared Enset fiber used to make the blades are shown in the **figure** below.

5.1.6 Mold Surface Preparation for Blade Manufacturing

The mold surfaces were polished and properly **CLEANED** before the blades were made. To guarantee simple demolding and reduce surface flaws, multiple layers of mold release wax were used, followed where needed by a polyvinyl alcohol (PVA) release agent.

A uniform gelcoat layer was then applied inside the mold cavity to improve surface finish and protect the composite from environmental degradation. **Figure** below shows the mold surface preparation and gelcoat application.

Figure 5.6: - Mold surface preparation applying JELCOAT and PVA for Release Purpose

5.1.7 Hand Lay-Up of Enset Fiber Composite Blade

After the gelcoat reached a tacky state, prepared Enset fiber layers were placed manually into the mold cavity following the predefined lay-up sequence. Resin mixed with the appropriate hardener was applied using the method of hand lay-up, which is largely used for low-cost composite blade manufacturing. Ensure the fiber wetting is complete, resulting in improved fiber matrix bonding. **Figure** below shows the hand lay-up process of Enset fiber and resin inside the blade mold.

A B C

Figure 5.7: - A=Fiber preparation, B= Resin application on Fiber, C= Completed Layer of Blade half

5.1.8 Mold Closing and Curing

Once the lay-up process was completed, the upper and lower mold halves were carefully aligned and clamped together. The composite blade was cured at ambient temperature for the duration recommended by the resin manufacturer, following standard composite curing practices. Figure below shows the closed mold during the curing process.

A B

Figure 5.8: - A= Mold half's joining, B= Mold Half connecting by bolts

5.1.9 Demolding and Edge Trimming

After full curing, the mold was opened and the blade was carefully removed. Excess material along the parting line was trimmed using hand tools, and the blade edges were sanded to restore the intended aerodynamic profile. Figure below shows the demolded blade before and after trimming.

A B

Figure 5.9: - A= Demolding, B= Opening the bolts

5.1.10 Surface Finishing and Protective Coating

The blade surface was progressively sanded using fine-grit abrasives to remove surface imperfections. A final protective coating or paint was applied to enhance resistance to moisture, ultraviolet radiation, and surface erosion, thereby improving long-term durability. **Figure** below shows the surface finishing and coating of the blade.

	
A	B

Figure 5.10: - A= Released blades, B= surface Finished Blade

The present study introduces a novel sustainable blade fabrication approach by integrating Enset (banana) fiber reinforcement with polyester resin, hardener, and protective gelcoat to produce a structurally viable small-scale wind turbine blade for rural electrification. Unlike conventional blades manufactured primarily from glass fiber composites, this research demonstrates the practical substitution of synthetic fibers with locally sourced Enset fiber while maintaining structural integrity through optimized resin–fiber ratio and proper curing with hardener. The application of gelcoat enhances surface finish, environmental resistance, and aerodynamic smoothness, contributing to improved durability and performance. The combined use of natural fiber reinforcement, controlled composite processing, and performance-based structural validation (maximum stress at root and acceptable displacement at tip) represents a new contribution toward cost-effective, environmentally friendly, and locally manufacturable wind turbine blade technology suitable for decentralized energy systems.

Figure5.11: The Assembly of the turbine blades

CHAPTER SIX

6. CONCLUSION AND RECOMMENDATIONS

6.1 Conclusion

This study detailed the design, manufacturing, and structural optimization of a small-scale horizontal-axis wind turbine blade composed of a polymer composite reinforced with Enset (false banana) fiber. SolidWorks Simulation was used to evaluate the structural performance under a number of design load cases indicative of regular operation, abnormal operation, and parked situations. The blade geometry was created using the SG6043 airfoil and modelled in SolidWorks.

Analysis using the Finite Element Method (FEM) revealed that the blade behaves structurally soundly under every load scenario examined. The maximal von Mises stress was localized at the blade root during normal operation, which is consistent with cantilever beam theory and validates proper load transmission to the hub. Maximum displacement occurred near the blade tip, as expected for a well-designed wind turbine blade, without exceeding allowable deflection limits.

Parked wind loading was found to be the leading design condition among the examined load situations, resulting in the greatest bending stress of roughly 4.07 MPa with a factor of safety of 7. Enset fiber composite's aptitude for withstanding axial loads was demonstrated by centrifugal loading at maximum rotational speed, which produced very low tensile stress and an exceptionally high factor of safety. The minimal safety standards advised for small-scale wind turbines were met by all load scenarios.

The results confirm that, when properly made and orientated, Enset fiber reinforced composite material may provide adequate strength, stiffness, and safety margins for applications of small wind turbine blade. Additionally, the combination of hand lay-up manufacturing and 3D-printed pattern for molds gives an affordable and regionally adaptable alternative for sustainable blade manufacture.

6.2 Recommendation for Future work

The study's conclusions lead to the following recommendations for further research and development:

1. **Experimental Validation:** - Physical testing such as static bending tests, fatigue tests, and vibration analysis should be undertaken to validate the numerical results produced from SolidWorks Simulation.
2. **Environmental Durability Study: -** Since natural fibers are sensitive to moisture, additional studies on water absorption, UV resistance, and surface coatings are recommended to enhance blade durability.
3. **Scaling and Field Testing: -** Field testing on an operational small-scale wind turbine is recommended to assess real-world performance and validate the design methodology.

Overall, the study demonstrates that Enset fiber composite is a promising, sustainable, and structurally viable material for small-scale wind turbine blade applications, particularly in regions where the fiber is locally available and cost-effective.

REFERENCES

1. Aravindhan N, Devan PK, Ponnuvel S, and Natarajan MP. A study of recent advancements and problems with small wind turbines in residential urban buildings. Environment and Energy. June 2, 2023; 34(4):1142–69.

2. Pinheiro E, Bandeiras F, Gomes M, Coelho P, Fernandes J. Evaluation of wind turbine and photovoltaic system performance in small-scale industrial settings. Reviews of Sustainable and Renewable Energy. August 2019, 110:392–401.

3. Troullaki K, Rozakis S, Latoufis K, Giotitsas C, Priavolou C, Freire F. Sustainable Rural Electrification: Harnessing a Cosmolocal Wind. Energies (Basel). 2022 Jun 25;15(13):4659.

4. Zhang Z, Liu X, Zhao D, Post S, Chen J. Overview of the development and application of wind energy in New Zealand. Energy and Built Environment. 2023 Dec;4(6):725–42.

5. Modelling and Aerodynamic Analysis of Small Scale, Mixed Aerofoil Horizontal Axis Wind Turbine Blades Kumar Gupta R, Purohit R, Warudkar V, Singh Rajpurohit S. In 2017, Mater Today Proc. 4(4):5370–84.

6. Wang H, Xiong B, Zhang Z, Zhang H, Azam A. Small wind turbines and their potential for internet of things applications. iScience. 2023 Sep;26(9):107674.

7. Andrawus JA, Watson J, Kishk M, and Adam A. Choosing an Appropriate Wind Turbine Maintenance Plan. Wind Engineering. Dec. 1, 2006; 30(6):471–86.

8. Federal Democratic Republic of Ethiopia Ministry of Water I and E (MWIE), E. Ethiopian Energy Policy and Strategy. Ministry of Water, Irrigation, and Energy (MWIE), Ethiopia. 2017.

9. TPNZAD and Kassahun Gashu Melese* RSR. SMALL SCALE WIND TURBINE BLADE DESIGN FOR ELECTRIFICATION IN RURRAL VILLAGES. Precision Technology International, Vol. 10, No. 1, 2021. 2021; 10.

10. Mishnaevsky L, Branner K, Petersen H, Beauson J, McGugan M, Sørensen B. Materials for Wind Turbine Blades: An Overview. Materials. 2017 Nov 9;10(11):1285.

11. Hejazi F, Firoozi AA, and Firoozi AA. A Comprehensive Analysis of Aerodynamic Optimisation in Wind Turbine Blade Design to Promote Wind Energy Efficiency. Basel Energies, June 13, 2024, 13:17(12):2919.

12. Bekele G, Palm B. Wind energy potential assessment at four typical locations in Ethiopia. Appl Energy. 2009 Mar;86(3):388–96.

13. Alemu YB, Tegegne EB. Wind as a Potential Alternative Energy Source in Ethiopia: Examining the Upper Blue Nile River Basin's Wind Energy Potential and Conducting a Feasibility Study for the Establishment of Wind Farms. 2024, pp. 229–58.

14. Thomas T, Prince A. Evolution of wind energy conversion system and recent challenges in grid integration: A review. IOP Conf Ser Mater Sci Eng. 2018 Aug 29;396:012051.

15. Innovations in Wind Turbine Blade Engineering: Examining Materials, Sustainability, and Market Dynamics Firoozi AA, Firoozi AA, Hejazi F. Sustainability, October 2, 2024, 16(19):8564.

16. Hannan MA, Al-Shetwi AQ, Mollik MS, Ker PJ, Mannan M, Mansor M, et al. Wind Energy Conversions, Controls, and Applications: A Review for Sustainable Technologies and Directions. Vol. 15, Sustainability (Switzerland). MDPI; 2023.

17. Anggoro RB, Setyobudi R, Sadrina A, Chalimah S, and Budi Satria MH. Solidworks Simulation-Based Design and Development of a Vertical Axis Wind Turbine with PVC Blades. Electrical and Computer Engineering Journal of Renewable Energy. Oct. 9, 2024; 4(2):150–8.

18. Alazrag A, Sbita L. Asynchronous Machine with Wind Turbine IRFO Control. WSEAS Transactions on Power Systems. 2022;17:141–54.

19. Lee KY, Cruden A, Ng JH, Wong KH. Variable designs of vertical axis wind turbines—a review. Vol. 12, Frontiers in Energy Research. Frontiers Media SA; 2024.

20. Savonius vs. Darrieus Rotor: A Comparative Analysis of Vertical Axis Wind Turbine Designs (Fazylova A, Alipbayev K, Aden A, Oraz F, Iliev T, Stoyanov I). inventions. Oct. 27, 2025; 10(6):95.

21. Anagnostou A. STUDY AND SIMULATION OF VERTICAL-AXIS WIND TURBINES. 2025.

22. Sengupta AR, Rakshit S, Majumder H. A comprehensive review on various approaches for performance improvement of Savonius wind turbines. Vol. 8, Discover Applied Sciences. Springer Nature; 2026.

23. Didane DH, Behery MR, Al-Ghriybah M, Manshoor B. A thorough review of recent developments in the design and performance analysis of vertical-axis wind turbines (VAWTs) [Online]. 2024. The manuscript is accessible at https://www.preprints.org/manuscript/202404.1310/v1

24. Aeroelastic Study of Downwind and Upwind Configurations Under Various Power Levels of Wind Turbines Sun Z, Sun Z, Xia Y, Shen W, Zhu W, Ferrer E. machines. July 1, 2025(7).

25. Hand B, Cashman A. A review on the historical development of the lift-type vertical axis wind turbine: from onshore to offshore floating application.

26. Theodossiou N, Li W, Tamburrino A, Lyberatos G, Yannopoulos SI, and Valipour M. Water raising devices, or pumps, have evolved over ages all across the world. Switzerland's water. 2015;7(9):5031–60.

27. Zarrabi M, Valibeig N. 3D modelling of an Asbad (Persian windmill): a link between vernacular architecture and mechanical system with a focus on Nehbandan windmill. Herit Sci. 2021 Dec 1;9(1).

28. Koetsier T. Windmills in The Netherlands. Advances in Historical Studies. 2025;14(01):16–35.

29. Möllerström E, Gipe P, Ottermo F. Wind power development: A historical review. Vol. 49, Wind Engineering. SAGE Publications Inc.; 2025. p. 499–512.

30. Dai J, Li M, Chen H, He T, Zhang F. Advances and difficulties in studying the blade load of big wind turbines. [Internet] Renew Energy. August 1, 2022 [cited January 26, 2026];196:482–96. https://www.sciencedirect.com/science/article/abs/pii/S0960148122010138?utm_-- is the source of this information.

31. Dai J, Li M, Chen H, He T, Zhang F. Advances and difficulties in studying the blade load of big wind turbines. [Internet] Renew Energy. August 1, 2022 [cited January 26, 2026];196:482–96. https://www.sciencedirect.com/science/article/abs/pii/S0960148122010138?utm_-- is the source of this information.

32. Wang L, Liu X, Kolios A. State of the art in the aeroelasticity of wind turbine blades: Aeroelastic modelling. Renewable and Sustainable Energy Reviews [Internet]. 2016 Oct 1 [cited 2026 Jan 26];64:195–210. Available from: https://www.sciencedirect.com/science/article/abs/pii/S1364032116302234?via%3Dihub

33. Sørensen JN. Aerodynamic aspects of wind energy conversion. Annu Rev Fluid Mech. 2011 Jan 21;43:427–48.

34. 9781315769981_previewpdf.

35. A comparison of dynamic inflow models for the blade element momentum technique was conducted by Mancini S, Boorsma K, Schepers G, and Savenije F. Wind Energy Science, Vol. 8. 2023; Copernicus Publications. pages 193–210.

36. Kaldellis JK, Tsesmelis M. Integrated energy balance analysis of a stand- alone wind power system for various typical Aegean Sea regions. Wind Energy. 2002 Jan;5(1):1–17.

37. Madsen HA, Voutsinas S, Sørensen N, Hansen MOL, and Sørensen JN. cutting edge of aerodynamics and aeroelasticity for wind turbines. Aerospace Sciences Progress [Internet]. June 1, 2006 [cited January 26, 2026];42(4):285–330. https://www.sciencedirect.com/science/article/abs/pii/S0376042106000649?via%3Dihub is the source source.

38. Kaldellis JK, Tsesmelis M. Integrated energy balance analysis of a stand- alone wind power system for various typical Aegean Sea regions. Wind Energy. 2002 Jan;5(1):1–17.

39. Corniglion R, Harris JC, Peyrard C. The aerodynamics of a blade pitch, rotor speed, and surge step for a wind turbine regarding dynamic inflow. Wind Energy. 2022 May 1;25(5):858–80.

40. Ferreira C, Van Kuik GAM, Yu W, and Hong VW. Engineering dynamic inflow models are validated using numerical and experimental methods. In: Conference Series, Journal of Physics. Institute of Physics Publications, 2016.

41. Ferreira C, Yu W, Sala A, Viré A. Dynamic inflow model for a floating horizontal axis wind turbine in surge motion. Wind Energy Science. 2022 Mar 8;7(2):469–85.

42. Yu W, Hong VW, Ferreira C, Van Kuik GAM. Validation of engineering dynamic inflow models by experimental and numerical approaches. In: Journal of Physics: Conference Series. Institute of Physics Publishing; 2016.

43. Oliveira HA, de Matos JG, Ribeiro LA de S, Saavedra OR, Vaz JRP. Evaluation of Correction Techniques Used in BEMT for Horizontal-Axis Wind Turbine Performance Prediction. Sustainability in the Swiss context. April 1, 2023, 15 (8).

44. Fernando N, Sanjimba S. Design and Simulation of an Optimized Small Wind Turbine.

45. Shen WZ, Mikkelsen R, Sørensen JN, Bak C. Tip loss corrections for wind turbine computations. Wind Energy. 2005;8(4):457–75.

46. Boatto U, Bonnet PA, Avallone F, Ragni D. Evaluation of engineering models for wind turbine rotors under uniform steady inflow based on Blade Element Momentum Theory. [Internet] Renew Energy. September 1, 2023 [cited January 26, 2026];214:307–17. https://www.sciencedirect.com/science/article/pii/S0960148123005001?via%3Dihub is the source of this information.

47. El Khchine Y, Sriti M. Tip Loss Factor Effects on Aerodynamic Performances of Horizontal Axis Wind Turbine. Energy Procedia [Internet]. 2017 Aug 1 [cited 2026 Jan 26];118:136–40. Available from: https://www.sciencedirect.com/science/article/pii/S1876610217325547?via%3Dihub

48. Wang L, Liu X, Kolios A. State of the art in the aeroelasticity of wind turbine blades: Aeroelastic modelling. Vol. 64, Renewable and Sustainable Energy Reviews. Elsevier Ltd; 2016. p. 195–210.

49. The dynamic stall model for wind turbine aerofoils was developed by Larsen JW, Nielsen SRK, and Krenk S. Structure of J Fluids [Internet]. October 1, 2007 [cited January 26, 2026];23(7):959–82. https://www.sciencedirect.com/science/article/abs/pii/S0889974607000291?utm_-- is the source of this information.

50. Bangga G, Lutz T, Arnold M. An improved second-order dynamic stall model for wind turbine airfoils. Wind Energy Science. 2020 Aug 20;5(3):1037–58.

51. Lee H, Sengupta B, Araghizadeh MS, Myong RS. Review of vortex methods for rotor aerodynamics and wake dynamics. Vol. 4, Advances in Aerodynamics . Springer; 2022.

52. pericles_1099182416.

53. Doosttalab M, Rautmann C, Ragni D, Ferreira CS, and Yu W. assessing dynamic stall models for the aerofoils of thick wind turbines. [Internet] Renew Energy. [cited 2026 Jan 26]; 260:125096; 2026 Mar 15. S0960148125027600?via%3Dihub is accessible at https://www.sciencedirect.com/science/article/abs/pii

54. Hu D, Hua O, Du Z. Stall-delay analysis for wind turbines with horizontal axes. [Internet] Renew Energy [May 1] [cited Jan. 26, 2026]; 31(6):821–3.ScienceDirect.com/science/article/abs/pii/S0960148105001199?utm_-- is the source of this information.

55. Gajendran MK, Ng EYK, Mehdizadeh A, and Syed Ahmed Kabir IF, Berrouk AS. Novel Machine-Learning-Based Stall Delay Correction Model for Improving Blade Element Momentum Analysis in Wind Turbine Performance Prediction. Wind. 2022 Dec 1;2(4):636–58.

56. Lanzafame R, Messina M. BEM theory: How to take into account the radial flow inside of a 1-D numerical code. Renew Energy [Internet]. 2012 Mar 1 [cited 2026 Jan 26];39(1):440–6. Available from: https://www.sciencedirect.com/science/article/abs/pii/S0960148111004514?utm_--

57. pericles_9780470686652.eae1112.

58. Pirrung G, Riziotis V, Madsen H, Hansen M, Kim T. Comparison of a coupled near- And far-wake model with a free-wake vortex code. Wind Energy Science. 2017;2(1):15–33.

59. Van Den Broek MJ, De Tavernier D, Hulsman P, Van Der Hoek D, Sanderse B, Van Wingerden JW. Free-vortex models for wind turbine wakes under yaw misalignment - a validation study on far-wake effects. Wind Energy Science. 2023 Dec 20;8(12):1909–25.

60. Kecskemety KM, Shaler K, and McNamara JJ. Benchmarking of a Free Vortex Wake Model for Prediction of Wake Interactions. Renew Energy [Internet]. 2019 Jun 1 [cited 2026 Jan 26];136:607–20. Available from: https://www.sciencedirect.com/science/article/abs/pii/S0960148118314757?utm_--

61. Su K, Bliss D. A novel hybrid free-wake model for wind turbine performance and wake evolution. Renew Energy [Internet]. 2019 Feb 1 [cited 2026 Jan 26];131:977–92. Available from: https://www.sciencedirect.com/science/article/abs/pii/S0960148118309054?utm_--

62. Wang L, Liu X, Kolios A. State of the art in the aeroelasticity of wind turbine blades: Aeroelastic modelling. Vol. 64, Renewable and Sustainable Energy Reviews. Elsevier Ltd; 2016. p. 195–210.

63. Sobotta D, Howell R, While A, Lou J, Sturge D.A hybrid actuator disc – Full rotor CFD methodology for modelling the effects of wind turbine wake interactions on performance. Renew Energy [Internet]. 2015 Aug 1 [cited 2026 Jan 26]; 80:525–37. Available from: https://www.sciencedirect.com/science/article/abs/pii/S096014811500169X?utm_--

64. Darling H, Schmidt DP. The Role of Fully Coupled Computational Fluid Dynamics for Floating Wind Applications: A Review. Vol. 17, Energies. Multidisciplinary Digital Publishing Institute (MDPI); 2024.

65. Sørensen JN. Aerodynamic aspects of wind energy conversion. Annu Rev Fluid Mech. 2011 Jan 21;43:427–48.

66. Yazar Soyadı YA, ALPMAN E, YILMAZ B, KODY S. Computational Studies of Horizontal Axis Wind Turbines Using Advanced Turbulence Models. MARMARA UNIVERSITY JOURNAL OF SCIENCE. 2014 Jun 30;2(26):36–36.

67. Rocha PAC, Rocha HHB, Carneiro FOM, Vieira da Silva ME, Bueno AV. k–ω SST (shear stress transport) turbulence model calibration: A case study on a small scale horizontal axis wind turbine. Energy [Internet]. 2014 Feb 1 [cited 2026 Jan 26];65:412–8. Available from: https://www.sciencedirect.com/science/article/abs/pii/S0360544213010207?utm_--

68. Rezaeiha A, Montazeri H, Blocken B. On the accuracy of turbulence models for CFD simulations of vertical axis wind turbines. Energy [Internet]. 2019 Aug 1 [cited 2026 Jan 26];180:838–57. Available from: https://www.sciencedirect.com/science/article/pii/S0360544219309168?utm_--

69. Jonkman J, Butterfield S, Musial W, Scott G. Definition of a 5-MW Reference Wind Turbine for Offshore System Development [Internet]. 2009. Available from: http://www.osti.gov/bridge

70. Ge L, Xie T, Yin J, Sun Z, Zhu WJ, Shen WZ. Study of blade torsional effect on the aerodynamic performance of wind turbine using a modal superposition method. Renew Energy [Internet]. 2026 Jan 1 [cited 2026 Jan 26];256:124084. Available from: https://www.sciencedirect.com/science/article/abs/pii/S0960148125017483?utm_--

71. Vázquez M, López V, Campos R, Cadenas E, Marin P. Structural and Modal Analysis of a Small Wind Turbine Blade Considering Composite Material and the IEC 61400-2 Standard. Energies (Basel). 2025 Feb 1;18(3).

72. Wang L, Liu X, Guo L, Renevier N, Stables M. A mathematical model for calculating cross-sectional properties of modern wind turbine composite blades. Renew Energy [Internet]. 2014 Apr 1 [cited 2026 Jan 26];64:52–60. Available from: https://www.sciencedirect.com/science/article/abs/pii/S0960148113005776

73. Camarena E, Anderson E. A critical verification of beam and shell models of wind turbine blades. Compos Struct [Internet]. 2025 Apr 1 [cited 2026 Jan 26];360:118999. Available from: https://www.sciencedirect.com/science/article/abs/pii/S0263822325001643?utm_--

74. Pardo D;, Branner K, Pardo DR. General rights Finite element analysis of the cross-section of wind turbine blades; a comparison between shell and 2D-solid models Finite Element Analysis of the Cross-section of Wind Turbine Blades; a comparison between shell and 2D-solid models. Downloaded from orbit.dtu.dk on. 2016.

75. Başakçılardan Kabakcı S, Şenlik A. End-of-life wind turbine blades as a resource: A comparative study of pyrolysis and combustion. J Anal Appl Pyrolysis [Internet]. 2025 Nov 1 [cited 2026 Jan 26]; 192:107308. Available from: https://www.sciencedirect.com/science/article/abs/pii/S0165237025003614?utm_--

76. Ennis BL, Das S, Norris RE. Economic competitiveness of pultruded fiber composites for wind turbine applications. Compos B Eng [Internet]. 2023 Oct 1 [cited 2026 Jan 27];265:110960. Available from: https://www.sciencedirect.com/science/article/abs/pii/S1359836823004638?utm_--

77. Amzil L, Fertahi S, Raffak T, Mouhib T. Towards sustainable blade design: A critical review of natural fiber-reinforced hybrid composites and structural analysis tutorials. Next Materials [Internet]. 2025 Jul 1 [cited 2026 Jan 27];8:100688. Available from: https://www.sciencedirect.com/science/article/pii/S2949822825002060?utm_--

79. Zhu-Enhancing-Tensile-Strength-in-Small-Wind-Turbine-Blades-Materials-and-Testing-Methods.

80. Chen S, Wang H, Wu Q, Zu L, Zhang Q, Zhang G, et al.Filament winding analysis and experimental verification of a combined revolution body with a concave surface. Compos Struct [Internet]. 2022 Jan 15 [cited 2026 Jan 27];280:114951. Available from: https://www.sciencedirect.com/science/article/abs/pii/S0263822321013829?utm_--

81. Knippers J, Früh N. Filament winding in multiple stages: Integrative design and fabrication method for fiber-reinforced composite components of complex geometries. Compos Struct [Internet]. 2021 Jul 15 [cited 2026 Jan 27];268:113969. Available from: https://www.sciencedirect.com/science/article/abs/pii/S0263822321004293?utm_--

82. Vargas-Rojas E. A comprehensive, prescriptive approach to the engineering of composite goods that emphasises structured design processes and the production process: review of a filament winding study. Compos B Eng [Online]. August 15, 2022 [cited January 27, 2026];243:110093. https://www.sciencedirect.com/science/article/abs/pii/S1359836822004693?utm_.

83. Sueda S, Keyser J, Li H. Calculating Filament Winding Paths with Friction and Concavities. [Internet] Computer-Aided Design. Dec. 1, 2021 [cited Jan. 27, 2026];141:103089. https://www.sciencedirect.com/science/article/abs/pii/S0010448521001007?utm.

84. Hernandez-Estrada E, Lastres-Danguillecourt O, Robles-Ocampo JB, Lopez-Lopez A, Sevilla-Camacho PY, Perez-Sariñana BY, et al. Considerations for the structural analysis and design of wind turbine towers: A review. Renewable and Sustainable Energy Reviews [Internet]. 2021 Mar 1 [cited 2026 Jan 27];137:110447. Available from: https://www.sciencedirect.com/science/article/abs/pii/S1364032120307346?utm_s

85. Hernandez-Estrada E. Lastres-Danguillecourt O, Robles-Ocampo JB, and Ibañez Duharte G. An experimental assessment of a new technique for frequency analysis of a small wind turbine with a tubular guyed tower. Engineering Structure [Online]. Nov. 15, 2023 [cited Jan. 27, 2026]; 295:116870. S0141029623012853?utm is accessible at https://www.sciencedirect.com/science/article/abs/pii_--

86. Chakrabarti S, Halkyard J, Capanoglu C. Historical Development of Offshore Structures. Handbook of Offshore Engineering (2-volume set). 2005;1–38.

87. Pourrajabian A, Rahgozar S, Dehghan M, and Akbari Jouchi A. A new and cost-effective rotor hub design for small wind turbines. Technologies and Evaluations for Sustainable Energy [Internet]. 2021 Oct 1 [cited 2026 Jan 27];47:101344. https://www.sciencedirect.com/science/article/abs/pii/S2213138821003544?utm is the online source._--

88. Eedara AK, Varanasi LNS. Constant and Variable Speed Wind Energy Conversion Systems. Encyclopedia of Renewable Energy, Sustainability and the Environment: Volume 1-4. 2024 Jan 1;3:437–46.

89. Eedara AK, Varanasi LNS. Constant and Variable Speed Wind Energy Conversion Systems. Encyclopedia of Renewable Energy, Sustainability and the Environment: Volume 1-4. 2024 Jan 1;3:437–46.

90. Olatayo KI, Stoker PW, and Wichers JH. Energy and economic performance of modest wind energy systems in South Africa's various climates. Reviews of Sustainable and Renewable Energy [Internet]. December 1, 2018 [cited January 27, 2026];98:376–92.

https://www.sciencedirect.com/science/article/abs/pii/S1364032118306853?utm is the source of this information._--

91. Simic Z, Havelka JG, Bozicevic Vrhovcak M. Small wind turbines – A unique segment of the wind power market. Renew Energy [Internet]. 2013 Feb 1 [cited 2026 Jan 27];50:1027–36. Available from: https://www.sciencedirect.com/science/article/abs/pii/S0960148112005083?utm_--

92. Jurasz J, Bochenek B, Wieczorek J, Jaczewski A, Kies A, Figurski M. Small-scale wind turbines' economic feasibility and energy potential. [Internet] Energy. May 1, 2025 [cited January 27, 2026]; 322:135608. https://www.sciencedirect.com/science/article/pii/S0360544225012502?utm_ is the source of this information.